B Cell Receptor–independent Stimuli Trigger Immunoglobulin (Ig) Class Switch Recombination and Production of IgG Autoantibodies by Anergic Self-Reactive B Cells

Tri Giang Phan,[1] Michelle Amesbury,[1] Sandra Gardam,[1] Jeffrey Crosbie,[1] Jhagvaral Hasbold,[2] Philip D. Hodgkin,[2] Antony Basten,[1] and Robert Brink[1]

[1]*Centenary Institute of Cancer Medicine and Cell Biology, Newtown NSW 2042, Australia*
[2]*Walter and Eliza Hall Institute for Medical Research, Parkville VIC 3050, Australia*

The Journal of Experimental Medicine

Abstract

In both humans and animals, immunoglobulin (Ig)G autoantibodies are less frequent but more pathogenic than IgM autoantibodies, suggesting that controls over Ig isotype switching are required to reinforce B cell self-tolerance. We have used gene targeting to produce mice in which hen egg lysozyme (HEL)-specific B cells can switch to all Ig isotypes (SW_{HEL} mice). When crossed with soluble HEL transgenic (Tg) mice, self-reactive SW_{HEL} B cells became anergic. However, in contrast to anergic B cells from the original nonswitching anti-HEL × soluble HEL double Tg model, self-reactive SW_{HEL} B cells also displayed an immature phenotype, reduced lifespan, and exclusion from the splenic follicle. These differences were not related to their ability to Ig class switch, but instead to competition with non-HEL–binding B cells generated by V_H gene replacement in SW_{HEL} mice. When activated in vitro with B cell receptor (BCR)-independent stimuli such as anti-CD40 monoclonal antibody plus interleukin 4 or lipopolysaccharide (LPS), anergic SW_{HEL} double Tg B cells proliferated and produced IgG anti-HEL antibodies as efficiently as naive HEL-binding B cells from SW_{HEL} Ig Tg mice. These results demonstrate that no intrinsic constraints to isotype switching exist in anergic self-reactive B cells. Instead, production of IgG autoantibodies is prevented by separate controls that reduce the likelihood of anergic B cells encountering BCR-independent stimuli. That bacteria-derived LPS could circumvent these controls may explain the well-known association between autoantibody-mediated diseases and episodes of systemic infection.

Key words: self-tolerance • autoimmunity • LPS • CD40 • hen egg lysozyme

Introduction

Ig transgenic (Tg)* mice expressing BCRs directed against endogenous or transgene-encoded self-antigens provide the opportunity to track the development of self-reactive B cells in vivo. Studies using such mice have revealed that self-tolerance in the B cell compartment can be maintained by silencing self-reactive B cells in several different ways. These include clonal deletion (1, 2), receptor editing (3, 4), and anergy (5) depending on the valency of the self-antigen and the site of its encounter with differentiating B cells.

Anergic self-reactive B cells have been characterized primarily using the anti–hen egg lysozyme (HEL) × soluble HEL double Tg model (MD4 Ig Tg × ML5 soluble HEL Tg mice). In this model, the induction of self-tolerance is accompanied by down-regulation of surface IgM (5), failure of B cells to colonize the splenic marginal zone (MZ; reference 6), inactivation of BCR signaling (7–9), and alterations in gene expression (10). Further analysis of the anti-HEL double Tg system has revealed an additional distinct fate for anergic B cells. This is evident in mixed bone marrow chimeras in which self-reactive MD4 B cells com-

Address correspondence to Robert Brink, Centenary Institute of Cancer Medicine and Cell Biology, Locked Bag Number 6, Newtown NSW 2042, Australia. Phone: 61-2-95656-136; Fax: 61-2-95656-105; E-mail: r.brink@centenary.usyd.edu.au

*Abbreviations used in this paper: BCM, B cell medium; BrdU, bromodeoxyuridine; CFSE, 5-(and 6-)carboxyfluorescein diacetate succinimidyl ester; CSR, class switch recombination; ES, embryonic stem; HEL, hen egg lysozyme; m.f.i., mean fluorescence intensity; MZ, marginal zone; NB6, non-transgenic C57BL/6; PALS, periarteriolar lymphoid sheath; SA, streptavidin; Tg, transgenic.

 J. Exp. Med. © The Rockefeller University Press • 0022-1007/2003/04/845/16 $8.00
Volume 197, Number 7, April 7, 2003 845–860
http://www.jem.org/cgi/doi/10.1084/jem.20022144

prise <20% of the B cell repertoire, instead of making up 90–95% of the repertoire as occurs in MD4 × ML5 double Tg mice (11). In these chimeras, anergic B cells do not enter the splenic follicle but accumulate at the follicular junction with the T cell–rich periarteriolar lymphoid sheath (PALS). Furthermore, the half-life of these B cells is reduced to <3 d (11). Two theories have been put forward to explain the altered migration and reduced lifespan of anergic B cells under these conditions. According to the first, anergic B cells cannot compete efficiently with nonself-reactive B cells for limited "niches" within the follicle that confer longer term survival (11, 12). However, significant reductions in the frequency of HEL-binding B cells can shift the antigen/BCR equilibrium toward higher levels of antigen binding by individual B cells, which raises the alternative possibility that more intense signaling by soluble self-antigen may cause the outer PALS arrest and reduced lifespan of anergic B cells (13). Because the interaction with self-antigen and frequency of HEL-binding B cells were not measured simultaneously in these studies (11–13), it remains to be resolved which of these potential mechanisms accounts for the altered behavior of anergic B cells.

A hallmark of B cell responses is the ability to vary the constant regions of expressed IgH by class switch recombination (CSR). Ig class switching has evolved to target different immune effector mechanisms toward invading pathogens. For instance, IgG but not IgM antibodies can penetrate tissues where they activate complement in situ and bind Fc receptors on macrophages and NK cells to induce antibody-dependent cellular cytotoxicity (14). Because of their ability to activate multiple immune effector systems, IgG autoantibodies pose a greater potential threat to the host than do IgM autoantibodies (15–19). This threat is exemplified by the relatively common finding of IgM but not IgG autoantibodies in sera from healthy individuals (20). Given the greater pathogenicity but reduced prevalence of IgG autoantibodies, self-reactive B cells may possess controls over Ig isotype switching in addition to any that normally act to prevent their differentiation into antibody-secreting cells.

Despite the insights gained from earlier Ig Tg models, it has not been possible to study the regulation of CSR by self-reactive B cells in detail because B cells from these models failed to undergo CSR. This problem has been overcome by using homologous recombination in embryonic stem (ES) cells to target rearranged V_HDJ_H genes to the 5′ end of the germline IgH gene (21). Location of the V_HDJ_H segment at its physiological position in the IgH locus results in a high frequency of B cells in the adult mouse expressing the targeted variable region (21–23). This frequency is typically lower than in conventional Ig Tg mice due to recombination of upstream V_H or V_H plus D segments into the targeted V_HDJ_H exon (22, 23). Nonetheless, B cells expressing a targeted heavy chain variable region can undergo CSR to all downstream isotypes in a physiological manner (21–23).

To combine the advantages of the well-characterized anti-HEL Ig Tg system with the ability to study CSR, we have targeted the V_H10 anti-HEL heavy chain variable region gene to the endogenous C57BL/6 IgH locus. SW_{HEL} mice carrying the targeted allele and an anti-HEL light chain transgene were shown to produce HEL-binding (HEL^+) B cells capable of switching to all classes of Ig. Additionally, a large population of non-HEL binding (HEL^-) B cells that had undergone V_H gene replacement was generated in these mice. These replacement events occurred in the absence of any obvious self-reactivity and may reflect instability of rearranged V_HDJ_H genes during early B cell development. When SW_{HEL} mice were crossed with ML5 soluble HEL Tg mice, the resulting self-reactive B cells became anergic. However, they also displayed an immature phenotype, reduced lifespan, and were excluded from the splenic follicle as well as the MZ, in contrast to the original MD4 double Tg model. Detailed analysis revealed that the changes observed in anergic SW_{HEL} B cells were not linked to their CSR potential but instead were due to competition from endogenous HEL^- B cells. Under normal circumstances, self-reactive B cells constitute a small proportion of the peripheral B cell repertoire and must compete with nonself-reactive B cells. The new SW_{HEL} model recapitulates this repertoire diversity and is therefore a more physiological system in which to study the fate of anergic self-reactive B cells and the effect of tolerance induction on regulation of CSR. When anergic self-reactive SW_{HEL} B cells were activated with BCR-independent stimuli in vitro, they proliferated and readily secreted isotype-switched anti-HEL Ig. These unexpected findings demonstrate that there is no intrinsic restriction to Ig class switching by anergic B cells and separate controls are required to prevent the secretion of IgG autoantibodies.

Materials and Methods

Mice. Tg mice were all maintained on a pure C57BL/6 background at the Centenary Institute Animal Facility. In MD4 Ig Tg mice the heavy (V_H10-μδ) and light chain ($V_κ10$-κ) transgenes encoding IgM and IgD with the high affinity anti-HEL specificity of the HyHEL10 mAb are cointegrated (5). In contrast, MD2 Ig Tg mice (24) carry only the V_H10-μδ heavy chain transgene and LC2 Ig Tg mice (produced by DNX Inc.) carry only the $V_κ10$-κ light chain transgene. Membrane-bound HEL was expressed as a neo self-antigen in KLK3 Tg mice under the control of the H2-K^b promoter (2) and soluble HEL was expressed under the control of either the metallothionein promoter (ML5 mice) or albumin promoter (AL3 mice). The latter two lines of mice express soluble HEL at intermediate (10–20 ng/ml) and high (80–160 ng/ml) concentrations, respectively (5, 13). Non-Tg C57BL/6 (NB6), C57BL/6-SJL.Ptprc^a (CD45.1 congenic), and BALB/c mice were obtained from the Animal Resources Centre (Canning Vale, Western Australia).

To produce anti-HEL Tg mice capable of undergoing CSR, the rearranged V_H10 variable region gene from the HyHEL10 hybridoma was targeted to the 5′ end of the endogenous IgH locus in mouse ES cells using the general approach of Taki et al. (see Fig. 1, A and B; reference 21). 5′ homology sequences for the targeting construct were obtained from a λ phage clone isolated from a C57BL/6 liver genomic DNA library (CLONTECH Laboratories, Inc.). 3′ homology sequences were ampli-

fied by PCR from C57BL/6 genomic DNA and verified by DNA sequencing. The final targeting construct included a loxP-flanked neomycin resistance cassette in reverse transcriptional orientation to the IgH locus that was located immediately 5′ to the rearranged V_H10 variable region and its associated promoter (see Fig. 1 C). ES cell electroporation, selection of homologous recombinant clones, and production of chimeric mice were performed using a C57BL/6 ES cell line (Bruce 4) as previously described (25). Two homologous recombinant clones were identified from 192 G418 resistant clones by PCR (see Fig. 1 D). Chimeric mice were generated from one of these clones and then backcrossed with C57BL/6 females. Black progeny heterozygous for the targeted V_H10 variable region ($V_H10_{tar}^{+/-}$; see Fig. 1 E) were mated with LC2 Ig Tg mice to produce SW_{HEL} mice heterozygous for both the V_H10_{tar} IgH allele and the $V_\kappa10$-κ Tg. All mice were screened for the presence of transgenes by PCR amplification of genomic DNA prepared from peripheral blood leukocytes.

Analysis of Heavy Chain Variable Region Expression. Spleen cells from SW_{HEL} mice were stained with anti–B220-PE and HEL-FITC, after which HEL- ($B220^+$, HEL^+) and non-HEL– ($B220^+$, HEL^-) binding B cells were separated to >95% purity by sorting on a FACStarPlus™ flow cytometer (BD Biosciences). $PolyA^+$ mRNA was prepared from 5×10^5 sorted cells using the Oligotex™ Direct mRNA Kit (QIAGEN). A modified 5′ rapid amplification of cDNA end system (GIBCO BRL) was used to generate PCR fragments for cloning and sequencing. $PolyA^+$ mRNA was reverse transcribed with a primer specific to the first constant region domain of the δ heavy chain ($C\delta_{H1}$) and the cDNA was then dC tailed with terminal deoxynucleotidyl transferase. Primary PCR amplification was performed with an unabridged anchor primer that recognized the poly-dC tail and a nested $C\delta_{H1}$-specific primer 5′ to the first primer. Secondary PCR amplification was performed with a universal primer to the first framework coding region and a third nested $C\delta_{H1}$-specific primer. The final PCR product was ligated with T4 DNA ligase (Roche Diagnostics) to the pCR2.1 plasmid (Invitrogen). Plasmid DNA was purified from individual clones and the inserts were sequenced (Australian Genome Research Facility).

Antibodies and Reagents. The following mAbs to murine antigens were purchased from BD Biosciences: anti–CD5-biotin (clone 53-7.3), anti–CD21/CD35-FITC (7G6), anti–CD23-PE (B3B4), anti–CD24-PE (M1/69), anti–CD45R/B220-biotin, -PerCP, and -APC (RA3-6B2), anti–CD45.1-PE (A20), anti–CD69-PE (H1.2F3), anti–CD86-PE (GL1), anti–IgM^b-PE (AF6-78), anti–IgD^b-PE (217-170), anti–IgD-FITC (11-26c.2a), anti–IgG1-biotin (A85-1), anti–IgG2a-biotin (R19-15), anti–IgG2b-biotin (R12-3), anti–IgG3-biotin (R40-82), anti–IgE-biotin (R35-118), anti–IgA-biotin (C10-1), and anti–Igκ-biotin (187.1). Anti–IgM-PE (1B4B1) and IgD-PE (11-26) were purchased from Southern Biotechnology Associates, Inc. HyHEL5, HyHEL9, anti-IgM (Bet-2), IgM^a (RS-3.1), and IgD^a (AMS-15.1) mAbs were purified from hybridoma supernatants and either biotinylated or conjugated to FITC as previously described (5). Conjugation to Alexa Fluor® 647 was performed using the Alexa Fluor® 647 Monoclonal Antibody Labeling Kit (Molecular Probes) according to the manufacturer's instructions. Streptavidin (SA)-PE, -PerCP, and -APC were purchased from BD Biosciences. HEL was purchased from Sigma-Aldrich and conjugated to FITC and Alexa Fluor® 647 as described above.

ELISAs. Anti-HEL antibody levels in sera and culture supernatants were measured by direct ELISA essentially as previously described (5). In brief, 96-well polystyrene plates (Nunc) were coated overnight at 4°C with HEL at 10 μg/ml. The wells were then blocked with 100 μL 1% BSA/PBS and serial dilutions of either sera or culture supernatants added together with the appropriate standards. Biotinylated isotype-specific mAb in 0.1% BSA/1% skim milk powder/PBS was used to detect bound antibody. SA-alkaline phosphatase (Roche Diagnostics) was then added and visualized with the substrate *p*-nitrophenyl phosphate (ICN Biomedicals). Absorbance at 405 nm was read and the concentration of anti-HEL antibodies was calculated from the standard curve.

Production of HyHEL10 Anti-HEL Ig Isotype Standards. Standards expressing the HyHEL10 specificity in association with each heavy chain isotype were produced by transiently transfecting Chinese hamster ovary cells with a $V_\kappa10$-κ light chain expression plasmid along with a heavy chain expression plasmid encoding V_H10 in association with secreted constant region sequences of either the μ, γ1, γ2a, γ2b, γ3, α, or ε heavy chain isotype. Constant region coding sequences were obtained by PCR amplification from C57BL/6 genomic DNA (IgH^b allotype) and verified by DNA sequencing. Supernatants were collected 3 d after transfection and the concentration of anti-HEL antibodies was determined by ELISA using a biotinylated anti-Igκ mAb and HyHEL10 ($IgG1^a$) purified from hybridoma supernatant as the standard.

Flow Cytometry. Four-color flow cytometry was performed on a dual laser FACSCalibur™ flow cytometer (BD Biosciences) and analyzed with CELLQuest™ v.3.3 software (BD Biosciences). Single cell suspensions of spleen, bone marrow, and peritoneal exudate were prepared and 10^6 cells were stained for surface markers in 96-well round-bottom plates and transferred to microtiter tubes (Bio-Rad Laboratories) for data acquisition. To reveal HEL-binding antigen receptors, cells were incubated initially with saturating concentrations of HEL (200 ng/ml) followed by biotinylated or fluorochrome-labeled HyHEL5 anti-HEL mAb (HyHEL5 and HyHEL10 mAbs bind HEL noncompetitively). To determine receptor occupancy, splenocytes were separately stained with anti–HEL-FITC (HyHEL5-FITC) with and without previous incubation with HEL. All data were gated on live lymphocytes on the basis of forward and side light scatter. For calculations of frequencies of HEL-binding B cells, the forward scatter was expanded because the high expression of anti-HEL receptors in MD4 and SW_{HEL} mice results in a proportion of these B cells forming doublets when stained with HEL plus HyHEL5.

For intracellular staining, cultured B cells were harvested and washed twice in 1% BSA/0.1% azide/PBS and fixed in 2% paraformaldehyde for 30 min at room temperature before permeabilization at 4°C overnight in 0.1% Tween20/0.1% azide/PBS. 10^6 cells were then washed and transferred to new round-bottom FACS® tubes (BD Biosciences) for staining with HEL-Alexa Fluor® 647 and biotinylated isotype-specific mAb revealed by SA-PE. Cell division number was determined from the 5-(and 6-)carboxyfluorescein diacetate succinimidyl ester (CFSE; Molecular Probes) peaks and gates were drawn around each peak to allow backgating ("division slicing") to determine the proportion of isotype-switched cells per division (26).

Bromodeoxyuridine (BrdU) Labeling. BrdU (Sigma-Aldrich) was included in the drinking water of the mice at a concentration of 0.25 mg/ml with the addition of 1% glucose as previously described (11, 27). After 3 d, splenocytes from treated and control mice were harvested and stained for cell surface markers. Cells were then fixed, permeabilized, and stained with anti–BrdU-

FITC (3D4) using the BrdU Flow Kit (BD Biosciences) according to the manufacturer's instructions. Proportions of $BrdU^+$ cells were determined with reference to equivalently stained cells from mice that were not administered BrdU.

Immunohistology. Spleens were snap frozen in liquid nitrogen and 5-μm sections were acetone fixed and air dried before staining as previously described (6). HEL binding was detected by staining with HEL at 200 ng/ml followed by polyclonal rabbit anti–HEL sera and revealed with sheep anti–rabbit IgG-FITC (Silenus Labs). The marginal sinus was identified by staining with purified anti–MadCAM-1 (MECA-367) rat mAb (BD Biosciences) followed by goat anti–rat IgG Texas red (Caltag Laboratories). To reveal the B cell area, sections were blocked with 1% rat serum (Jackson ImmunoResearch Laboratories) and then exposed to biotinylated anti-B220 and SA-FluoroBlue (Biomeda).

Bone Marrow Chimeras. 10–16-wk-old recipient mice were lethally irradiated (950 rads) and rescued 6–8 h later by intravenous injection with 2×10^7 bone marrow cells. All mice were analyzed 2–3 mo after reconstitution.

In Vitro Cultures. The ability of B cells to respond to BCR engagement was measured in vitro by culturing fresh splenocytes overnight at 37°C in B cell medium (BCM) containing RPMI 1640 medium supplemented with 10% heat-inactivated FCS (Life Technologies), 2 mM L-glutamine, 1 mM sodium pyruvate, 0.1 mM nonessential amino acids, 10 mM Hepes, 100 U/ml penicillin, 100 μg/ml streptomycin, and 5×10^{-5} M 2-ME (all from Sigma-Aldrich) with and without HEL at a concentration of 500 ng/ml. Cells were then surface stained to detect up-regulation of CD86 and CD69 by flow cytometry.

B cell responses to BCR-independent stimuli were determined by activating purified small B cells in vitro with either 5 μg/ml agonist anti-CD40 mAb (HM40-3; BD Biosciences) or CD40L prepared from Sf9 insect cell line transfected with a baculovirus vector containing CD40L (provided by M.R. Kehry, Boehringer Ingelheim, Ridgefield, CT) plus 10 ng/ml IL-4 (Sigma-Aldrich) to simulate T cell–derived signals or 2.5 μg/ml LPS (Sigma-Aldrich) to simulate T-independent signals. Small B cells were purified from spleens as described previously (28). RBCs were lysed with hypotonic ammonium chloride and adherent cells were depleted by incubation on a plastic tissue culture dish. T cells were depleted by complement-mediated lysis using CD4- (RL172), CD8- (31M), and Thy.1- (30-H12) specific hybridoma supernatants. B cells were further purified by Percoll (Amersham Biosciences) density gradient and small B cells were recovered from the 65/80% interface. The recovered B cells were >90% pure as determined by flow cytometry. Initially, cells were washed and resuspended in 0.1% BSA/PBS at 10^7 cells/ml and labeled with CFSE at a final concentration of 5 μM for 10 min at 37°C. Unlabeled CFSE was quenched with ice-cold RPMI 1640 medium containing 10% FCS (Commonwealth Serum Laboratories) and washed twice with BCM. The labeled cells were then cultured in BCM and appropriate stimuli for 3–4 d.

Results

Generation of SW_{HEL} Mice. To produce mice in which B cells have the same anti-HEL specificity as the MD4 Ig Tg line but can undergo CSR, we generated two new lines of mice. The first of these lines, LC2 Ig Tg mice, carried the same $V_\kappa 10$-κ light chain transgene present in MD4 mice (5) but without the accompanying $V_H 10$-μδ heavy chain transgene. For the second line, gene targeting in ES cells was used to insert the rearranged $V_H 10$ exon in place of the J_H segments at the 5′ end of the endogenous IgH gene (Fig. 1, A and B). The LC2 Ig Tg and $V_H 10_{tar}$ gene-targeted mice were produced on an inbred C57BL/6 background identical to that of MD4. When heterozygous $V_H 10_{tar}$ and LC2 Ig Tg mice were mated, the two loci were inherited at the expected Mendelian ratios. Mice heterozygous for both loci ($V_H 10_{tar}{}^{+/-} \times$ LC2) were designated SW_{HEL}.

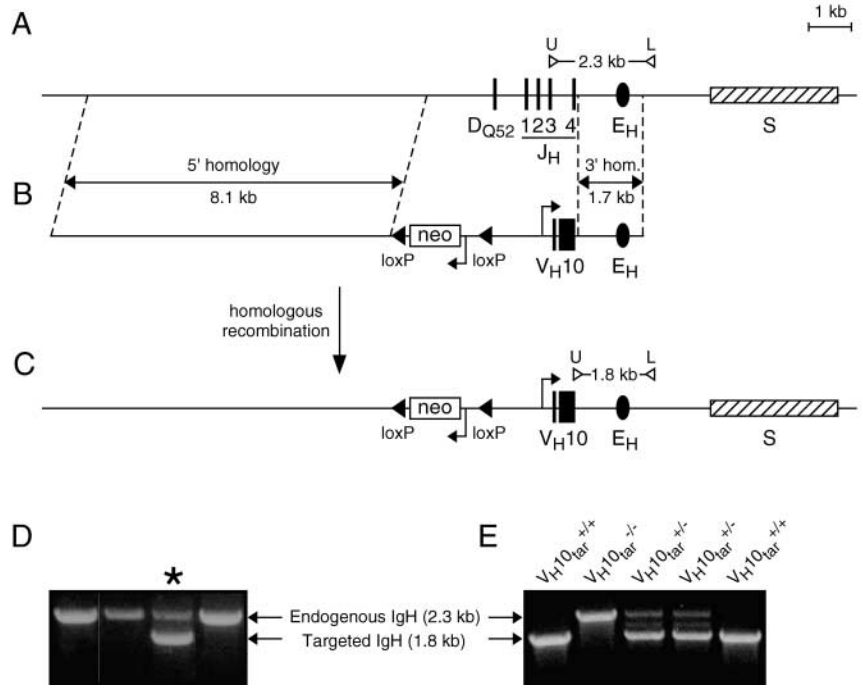

Figure 1. Targeted insertion of the anti-HEL $V_H 10$ variable region gene into the C57BL/6 IgH gene. (A) Endogenous IgH locus indicating the location of screening primers located within the $J_H 3$ segment and 3′ of the IgH intronic enhancer (E_H). U, upper primer; L, lower primer. (B) Targeting construct indicating 5′ and 3′ homology arms and the inverted loxP-neo^r-loxP cassette and rearranged $V_H 10$ variable region gene replacing DQ52 and all four J_H segments of the endogenous IgH gene. Square arrows indicate promoters associated with neo^r and $V_H 10$. (C) Targeted IgH locus ($V_H 10_{tar}$) after homologous recombination. $V_H 10$ utilizes $J_H 3$ and therefore hybridizes with the upper primer described above. Due to deletion of $J_H 4$, amplification of the targeted locus results in a shorter PCR product than that from the endogenous heavy chain gene (1.8 vs. 2.3 kb). (D) PCR screening of DNA from G418-resistant ES cell clones obtained after transfection with the targeting construct. A single homologous recombinant heterozygous for $V_H 10_{tar}$ is shown (*). (E) PCR screening of mice derived from homologous recombinant ES cells. Heterozygous ($V_H 10_{tar}{}^{+/-}$) mice were mated and DNA from the blood of the resulting litter was PCR amplified with the upper and lower screening primers described above.

SW_{HEL} Mice Contain both HEL-binding B Cells and non-HEL–binding B Cells Generated by V_H Gene Replacement. Flow cytometric analysis of spleen cells from LC2, $V_H10_{tar}{}^{+/-}$, and SW_{HEL} ($V_H10_{tar}{}^{+/-}$ × LC2) mice confirmed that expression of both HyHEL10 heavy and light chain variable regions is required to generate significant numbers of B cells with BCRs capable of binding HEL (Fig. 2 A). Although a high proportion (40–60%) of B cells in SW_{HEL} mice bound HEL, this was significantly lower than the frequency of >90% routinely observed in MD4 Ig Tg mice (Fig. 2 A). The difference was not due to inefficient expression of the $V_\kappa10$-κ transgene by SW_{HEL} mice because inheritance of the same $V_\kappa10$-κ transgene in conjunction with the V_H10-μδ transgene (MD2 × LC2 mice) resulted in high frequencies of HEL^+ B cells similar to those observed in MD4 (not depicted).

The failure of HEL^- B cells from SW_{HEL} mice to express the targeted allele raised the possibility that this was due to V_H gene replacement of the V_H10 exon. V_H gene replacement has been reported in other mice carrying targeted IgH alleles whereby the V_H segment of the targeted V_HDJ_H exon is replaced by upstream V_H or V_H plus D elements during early B cell development (22, 23). To confirm this, HEL^+ and HEL^- B cells from SW_{HEL} mice were isolated to >95% purity by FACS® sorting. PCR analysis of purified genomic DNA showed that the neo^r selection marker located 5′ of the targeted V_H10 exon (Fig. 1 C) was deleted from HEL^- but not HEL^+ B cells (not depicted), consistent with recombination of upstream V_H/V_H plus D elements specifically in the HEL^- B cells. RT-PCR cloning and sequencing of heavy chain variable region genes present in mature δ heavy chain mRNAs detected only unaltered V_H10 variable regions in HEL^+ B cells (Table I). In contrast, about half (9 out of 21) of the cDNA clones derived from HEL^- B cells expressed hybrid variable region exons consisting of the D and J_H segments of the targeted V_H10 exon recombined in frame with upstream V_H plus D sequences whereas 11 out of 21 clones expressed V_HDJ_H exons derived from the nontargeted IgH allele (the single unaltered V_H10 clone from the sorted HEL^- B cell population was presumably derived from one of the ~5% contaminating HEL^+ B cells; Table I). Flow cytometric analysis of spleen cells from SW_{HEL} mice on a C57BL/6 × BALB/c (IgH^b × IgH^a) F1 genetic background confirmed that HEL^+ B cells expressed only the targeted IgH^b allele (Table I). Consistent with the sequencing results, approximately equal proportions of the HEL^- B cells expressed either the targeted IgH^b or the nontargeted IgH^a allele (Table I). The fact that heavy chain allelic exclusion was maintained in the HEL^- B cell population indicated that rearrangement and expression of the nontargeted allele occurred only when a nonproductive V_H replacement event had taken place at the targeted IgH allele.

HEL^+ SW_{HEL} B Cells Belong to the B2 Lineage and Mature Normally. Analysis of naive splenic B cells by flow cytometry revealed that the HEL^+ B cells from SW_{HEL} mice have an IgM^{hi} $IgD^{lo\text{-}hi}$ antigen receptor phenotype identical to that of MD4 Ig Tg B cells (Fig. 2 B). By contrast, HEL^- SW_{HEL} B cells have the same BCR phenotype as wild-type B cells, including the IgM^{lo} IgD^{hi} subset lacking in the HEL^+ B cell populations from SW_{HEL} and MD4 mice (Fig. 2 B). Despite the differences in BCR phenotype between HEL^+ and HEL^- B cells, expression of non-Ig maturation markers and localization to anatomical compartments

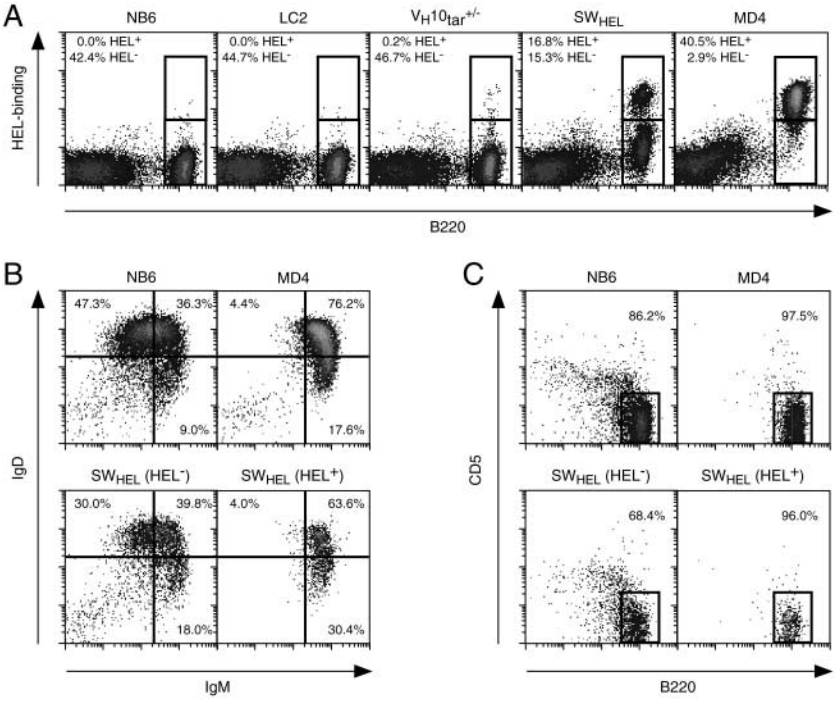

Figure 2. Phenotypic characterization of B cells from SW_{HEL} mice. (A) Spleen cells from 10–14-wk-old NB6, LC2, $V_H10_{tar}{}^{+/-}$, SW_{HEL} ($V_H10_{tar}{}^{+/-}$ × LC2), and MD4 Ig Tg mice were harvested and stained with anti–B220-APC, HEL plus anti–HEL-FITC, anti–IgD-PE, and anti–IgM-biotin plus SA-PerCP. Cells were analyzed by flow cytometry and the frequency of HEL^+ (top box) and HEL^- (bottom box) B cells in each density plot was indicated. Values from each mouse are representative of more than five independent experiments. (B) Spleen cells were stained as for A. IgM and IgD expression data are displayed for all $B220^+$ B cells (NB6 and MD4, top) or specifically for HEL^+ and HEL^- B cells (SW_{HEL}, bottom) using the gates shown in A. Numbers indicate the proportions of gated cells within the indicated quadrants. Data are representative of more than five independent experiments. (C) Cells were isolated by peritoneal lavage from the indicated mice and stained with anti–B220-APC, HEL plus anti–HEL-FITC, anti–IgM-PE, and anti–CD5-biotin plus SA-PerCP. Cells were analyzed by flow cytometry and gated on live cells that were $B220^+$ and/or IgM^+ to include both the B1 and B2 cell populations. For SW_{HEL} mice the peritoneal cavity B cells were further gated into HEL^+ and HEL^- subpopulations. Numbers indicate the proportion of gated cells in the $B220^{hi}$ $CD5^-$ window. Data are representative of three independent experiments.

Table I. *IgH Expression by HEL$^+$ and HEL$^-$ Splenic B Cells from SW$_{HEL}$ Mice*

	HEL$^+$ B cells	HEL$^-$ B cells
IgH V-region expression[a]		
Intact V_H10	10/10	1/21
Disrupted V_H10	0/10	9/21
Endogenous IgH allele	0/10	11/21
IgH allotype expression[b]		
Targeted allotype (IgH^b)	99.6 ± 0.1%	52.5 ± 1.3%
Endogenous allotype (IgH^a)	0.4 ± 0.1%	47.5 ± 1.3%

[a]To analyze IgH V-region expression, SW$_{HEL}$ spleen cells were stained with anti–B220-PE and HEL-FITC, and HEL$^+$ and HEL$^-$ splenic B cells (refer to Fig. 2 A) were separated to >95% purity by FACS® sorting. RT-PCR, cloning, and sequencing of δ heavy chain cDNA clones was performed and the number of clones expressing the intact targeted V_H10 allele, disrupted V_H10 allele that had undergone V_H region replacement, and endogenous IgH allele was determined. The denominator indicates the total number of clones isolated for each group. [b]SW$_{HEL}$ (IgH^b) mice were crossed with non-Tg BALB/c (IgH^a) mice and spleen cells from SW$_{HEL}$ F1 progeny stained with anti–B220-APC, HEL plus anti–HEL-FITC, anti–IgM^a-PE, and anti–IgM^b-biotin plus SA-PerCP. The proportions of HEL$^+$ and HEL$^-$ B cells that stained for IgM^a or IgM^b were calculated separately for each mouse. Percentages represent mean ± SD for four mice.

within the spleens of SW$_{HEL}$ mice were similar. Thus, HEL$^+$ and HEL$^-$ B cells both contained normal proportions of cells with immature, follicular, and MZ phenotypes as defined by expression of CD21/CD35 and CD23 (see Fig. 6 A; not depicted) and both populations localized to the follicle and MZ of the spleen (see Fig. 5 D).

Analysis of cells obtained by peritoneal cavity lavage indicated that HEL$^+$ SW$_{HEL}$ B cells mirror the behavior of MD4 B cells in their failure to differentiate along the B1 cell lineage. Accordingly, HEL$^+$ B cells belong to the conventional B2 cell lineage, with B1 lineage (B220^{lo} CD5$^{+/-}$) cells in SW$_{HEL}$ mice residing within the HEL$^-$ B cell pool (Fig. 2 C).

HEL$^+$ SW$_{HEL}$ B Cells Can Switch to all Ig Isotypes. Sera from nonimmunized MD4 Ig Tg mice contain >10 μg/ml anti-HEL IgM antibody (Fig. 3 A; reference 5). When tested for the presence of class-switched antibodies, MD4 mice were also found to have detectable, albeit low, levels of anti-HEL IgG2b, IgG3, and IgA in their sera (Fig. 3 A), presumably due to rare interchromosomal CSR events that have been reported in other Ig Tg models (29). By contrast, sera from nonimmunized SW$_{HEL}$ mice contained anti-HEL antibodies of all isotypes (Fig. 3 A) with the exception of IgE (not depicted). Because IgE is typically present in mouse serum at 1,000-fold lower levels than other isotypes, we tested for IgE production by stimulating SW$_{HEL}$ B cells in vitro with CD40L plus IL-4. Stimulation with LPS was used as a control. Not only were SW$_{HEL}$ B cells shown to secrete anti-HEL IgE in response to CD40L plus IL-4, but the different classes of anti-HEL antibody produced by these cells (Fig. 3 B) corresponded to those typically secreted by non-Tg B cells under the same conditions (30, 31). Thus, HEL$^+$ SW$_{HEL}$ B cells produced IgG1 and IgE but not IgG2b nor IgG3 in response to CD40L plus IL-4 and vice versa for LPS (Fig. 3 B). HEL$^+$ MD4 B cells, on the other hand, produced negligible quantities of class-switched antibodies under both conditions.

Exposure to Soluble HEL As a Neo Self-Antigen Induces Anergy in HEL$^+$ SW$_{HEL}$ B Cells. Having established that HEL$^+$ SW$_{HEL}$ B cells undergo CSR normally, we sought to determine the effects of self-reactivity on this process. In the MD4 nonswitching model, HEL$^+$ B cells produced in mice expressing membrane-bound HEL fail to enter peripheral lymphoid tissues and are deleted in the bone marrow (2). Similarly, self-reactive HEL$^+$ SW$_{HEL}$ B cells were deleted in the bone marrow of irradiated membrane HEL Tg mice reconstituted with SW$_{HEL}$ bone marrow (not depicted). Thus, the ability to undergo CSR does not affect the deletion of high avidity self-reactive B cells in the bone marrow.

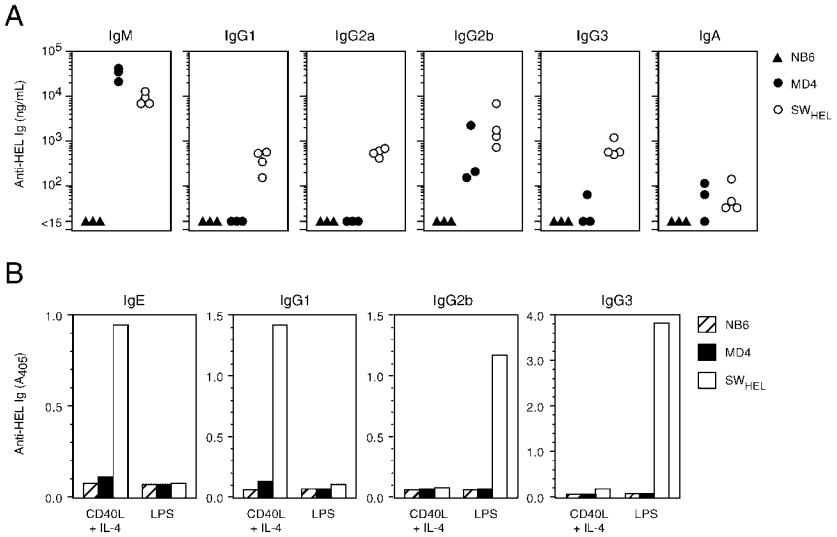

Figure 3. Ig class switching by SW$_{HEL}$ HEL$^+$ B cells. (A) Constitutive production of anti-HEL Ig by NB6, MD4, and SW$_{HEL}$ mice. Serum were obtained from 8–12-wk-old mice and the concentration of anti-HEL Ig isotypes was quantitated by ELISA. (B) In vitro production of anti-HEL Ig by NB6, MD4, and SW$_{HEL}$ splenic B cells. Small, resting splenic B cells were purified from 8–12-wk-old NB6, MD4, and SW$_{HEL}$ mice and stimulated in vitro with either CD40L plus IL-4 or LPS. Culture supernatants were harvested after 4 d and analyzed for the presence of anti-HEL Ig using isotype-specific secondary antibodies. Precise antibody concentrations were not calculated and the data are expressed as the absorbance readings obtained from neat culture supernatants. Data are representative of two independent experiments.

Of more relevance to the regulation of isotype-switched autoantibody production is the scenario where anergic self-reactive B cells with the capacity to undergo CSR colonize peripheral lymphoid tissues. To study this, the development and responsiveness of self-reactive SW_{HEL} and MD4 B cells were compared in double Tg mice expressing intermediate (ML5) or high (AL3) levels of soluble HEL. As previously demonstrated, HEL^+ B cells are not deleted in MD4 × ML5 mice (Fig. 4 A) but become anergic. This is manifested by down-regulation of surface IgM (not depicted), greatly reduced secretion of anti-HEL IgM (Fig. 4 C), and the inability to up-regulate CD86, CD69, or increase cell size in response to stimulation with HEL in vitro (Fig. 4 D and not depicted). A very similar picture was observed in MD4 × AL3 mice that expressed higher levels of soluble HEL (Fig. 4 and not depicted). When SW_{HEL} mice were crossed with ML5 mice, the frequency of self-reactive HEL^+ B cells was reduced compared with that in SW_{HEL} mice (Fig. 4 A). Although such a decrease was not observed in either MD4 × ML5 nor MD4 × AL3 mice, the induction of anergy in self-reactive SW_{HEL} × ML5 B cells otherwise appeared to be similar to that in the two MD4 double Tg combinations. Thus, self-reactive SW_{HEL} B cells exhibited the IgM^{lo} phenotype characteristic of anergic B cells (Fig. 4 B), secreted little anti-HEL Ig of any isotype in vivo (Fig. 4 C), and were unable to up-regulate CD86, CD69, or increase in size after antigenic stimulation in vitro (Fig. 4 D and not depicted). Therefore, the ability to undergo CSR does not appear to affect the induction of anergy to soluble self-antigen in SW_{HEL} B cells.

Self-reactive SW_{HEL} B Cells Display an Immature Phenotype and Impaired Migration to the Splenic Follicle and MZ. Analysis of surface expression of the CD21/CD35 and CD23 molecules allowed immature ($CD21/CD35^{lo}$ $CD23^{lo}$), mature follicular ($CD21/CD35^{int}$ $CD23^{hi}$), and MZ ($CD21/CD35^{hi}$ $CD23^{lo}$) B cell subpopulations to be resolved within the spleen (32–34). In the absence of self-antigen, the proportions of MD4 and SW_{HEL} HEL^+ B cells exhibiting the three phenotypes were comparable to those seen in non-Tg splenic B cells (Fig. 6 A). Correspondingly, HEL^+ B cells were located in both the follicle and MZ of spleens from MD4 (6) and SW_{HEL} mice (Fig. 5, A and D). In MD4 double Tg mice, very few HEL^+ B cells displayed the MZ phenotype (Fig. 6 A), consistent with previous histological analyses showing that the MZ is poorly developed in these mice and consists almost exclusively of rare HEL^- B cells (Fig. 5, B and C; reference 6). In contrast to the MZ, the immature and follicular splenic B cell subpopulations varied little between MD4 single and double Tg mice when analyzed by immunohistology (Fig. 5, A, B, and C) and flow cytometry (Fig. 6 A).

Histological analysis of SW_{HEL} × ML5 mice not only confirmed the reduction in numbers of splenic HEL^+ B cells compared with SW_{HEL} mice (Fig. 5, D and E), but also illustrated differences in their migratory properties. Thus, HEL^+ B cells in SW_{HEL} × ML5 mice do not efficiently col-

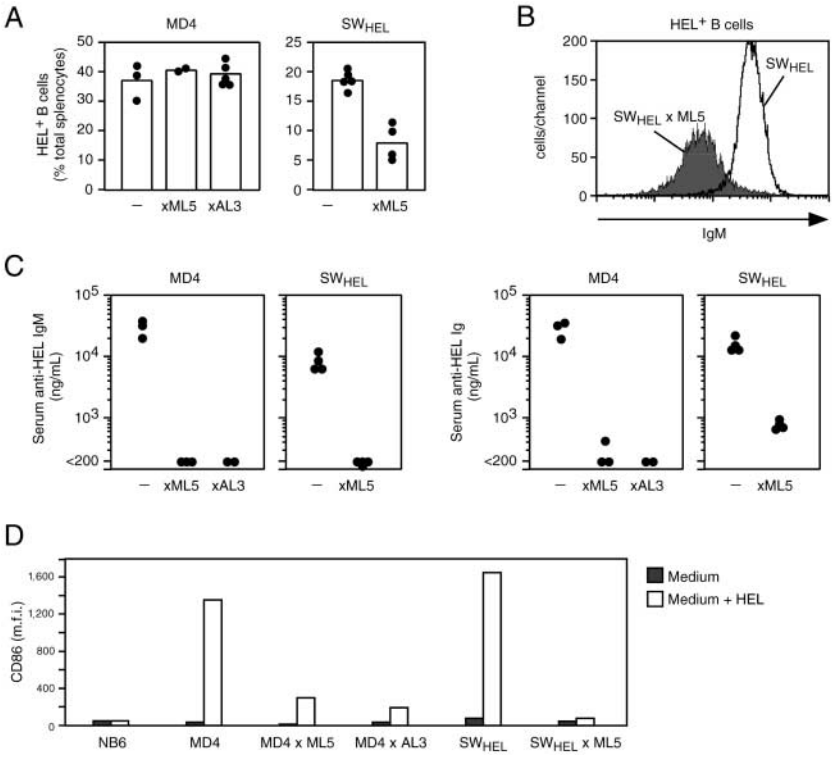

Figure 4. Induction of anergy in SW_{HEL} double Tg mice. (A) Reduced frequency of HEL^+ B cells in SW_{HEL} × ML5 but not MD4 × ML5 nor MD4 × AL3 mice. Spleens from 8–14-wk-old mice of the indicated genotypes were harvested and stained for B220 and HEL binding as in Fig. 2 A. HEL^+ B cells were quantitated as a proportion of total splenocytes. Columns indicate the mean of the individual data points. Dashes on the x axis indicate data from MD4 or SW_{HEL} mice not expressing HEL. (B) SW_{HEL} × ML5 HEL^+ B cells down-regulate surface IgM expression. Spleen cells from SW_{HEL} and SW_{HEL} × ML5 littermates were stained for B220, HEL binding, and IgM as described in Fig. 2. Overlayed histograms indicate IgM fluorescence of HEL^+ B cells. The data are representative of four pairs of similarly analyzed littermates. (C) Reduced production of anti-HEL antibodies in SW_{HEL} × ML5 mice. Sera from 8–14-wk-old mice of the indicated genotypes were analyzed by ELISA for anti-HEL IgM and total anti-HEL Ig using anti-IgM and anti-Igκ secondary antibodies, respectively. In each case the data were quantitated against an HyHEL10 IgM standard. Dashes on the x axis indicate data from MD4 or SW_{HEL} mice not expressing HEL. (D) SW_{HEL} × ML5 HEL^+ B cells have inactive BCR signaling. Spleen cells from 8–10-wk-old mice of the indicated genotypes were cultured for 24 h in the presence or absence of 500 ng/ml HEL and then stained with anti–B220-PerCP, HEL plus anti–HEL-FITC, and anti–CD86-PE. Relative CD86 levels were obtained by gating either on total $B220^+$ B cells (NB6) or HEL^+ B cells (all other mice) and calculating the mean fluorescence intensity (m.f.i.) of CD86 staining. Similar results were obtained in an independent experiment.

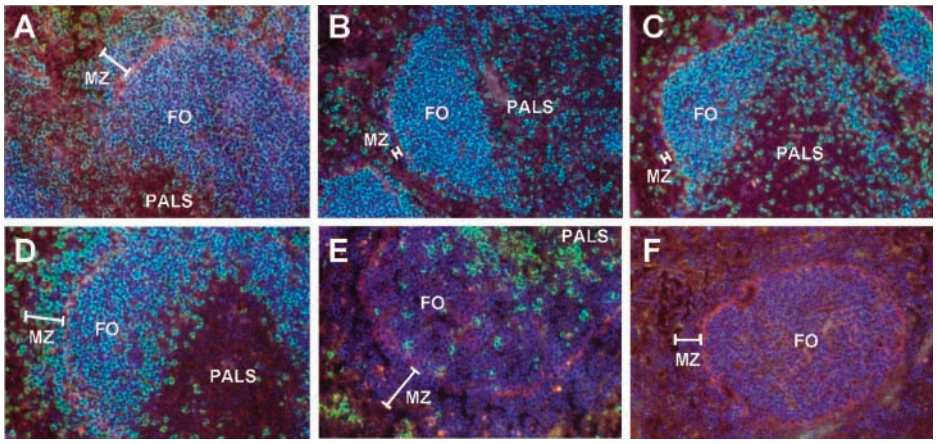

Figure 5. Anatomical localization of nontolerant and anergic B cells in the spleens of MD4 and SW_{HEL} mice. Immunofluorescent staining was performed on spleen sections from the following 9–12-wk-old mice: (A) MD4, (B) MD4 × ML5, (C) MD4 × AL3, (D) SW_{HEL}, (E) SW_{HEL} × ML5, and (F) NB6. B cells were stained purple (anti–B220-biotin plus SA-FluoroBlue) and HEL binding BCRs were stained green (HEL plus rabbit polyclonal anti–HEL plus anti–rabbit IgG-FITC). HEL^+ B cells overlay purple and green and therefore appear cyan whereas HEL^- B cells are purple. Immature HEL^+ B cells express low levels of B220 and therefore appear greener than mature B cells. The marginal sinus was stained red (anti–MadCAM-1 plus anti–rat IgG-Texas red) to delineate the MZ (bar) and the inner follicle (FO). The T cell–rich PALS is also shown. Note the thin MZ in MD4 × ML5 and MD4 × AL3 mice made up predominantly of HEL^- B cells (B and C) and the concentration of immature HEL^+ B cells in the border between the follicle and the PALS in SW_{HEL} × ML5 mice (E). The section from the non-Tg NB6 mouse (F) is distal to the central arteriole and therefore does not show the PALS. Data from flow cytometric analysis of the same mice are shown in Fig. 6, A and B. Similar data were obtained from independently analyzed mice of the same genotypes.

onize either the splenic MZ nor follicle, but instead localize near the boundary between the PALS and the follicle (Fig. 5 E). Flow cytometric analysis revealed that few HEL^+ B cells from SW_{HEL} double Tg mice display the CD21/$CD35^{hi}$ $CD23^{lo}$ MZ phenotype. Moreover, the frequency of CD21/$CD35^{int}$ $CD23^{hi}$ follicular B cells is reduced compared with SW_{HEL} mice (Fig. 6 A). Conversely, the proportion of anergic HEL^+ SW_{HEL} × ML5 B cells with an immature CD21/$CD35^{lo}$ $CD23^{lo}$ phenotype is greatly increased (Fig. 6, A and C), which clearly distinguishes them from MD4 double Tg B cells. Identification of immature B cells on the basis of CD24 (HSA) and CD21/CD35 expression (CD21/$CD35^{lo}$ $CD24^{hi}$) gave similar results to those obtained using CD23 and CD21/CD35 (not depicted).

Failure of Anergic SW_{HEL} Double Tg B Cells to Mature and Localize to the Follicle Is Not Due to Increased BCR Occupancy by Self-Antigen. One interpretation of the results described above is that the ability to undergo CSR may cause self-reactive B cells to be more readily purged from the mature B cell repertoire. However, interaction with increased levels of self-antigen as well as competition with nonself-reactive B cells have previously been claimed to influence the fate of anergic B cells (11–13), raising the possibility that variability in one or both of these parameters could explain the different maturation and migration patterns of self-reactive B cells in SW_{HEL} versus MD4 double Tg mice. To distinguish between these possibilities, we initially compared the levels of BCR occupancy by self-antigen between the HEL^+ B cell populations from the various double Tg mice. As expected, the proportion of BCRs occupied by HEL on B cells from SW_{HEL} × ML5 mice (70–80%) was greater than MD4 × ML5 mice (40–50%) due to the presence of fewer B cells capable of binding available HEL (Fig. 6 B). MD4 × AL3 B cells, however, exhibited significantly higher levels of receptor occupancy (90–100%; Fig. 6 B). Therefore, simultaneous analysis of receptor occupancy and B cell maturity clearly showed that the failure of self-reactive SW_{HEL} × ML5 B cells to mature could not be explained by greater interaction with self-antigen (Fig. 6 C).

The alternative possibility that self-reactive SW_{HEL} × ML5 B cells exhibited impaired migration and maturation due to competition from nonself-reactive B cells was consistent with the data obtained. Thus, HEL^- B cells were more prevalent in SW_{HEL} double Tg mice (60–80% of B cells) than in MD4 double Tg mice (<10% of B cells; Fig. 6 B). Nevertheless, a possible role for intrinsic differences between anergic SW_{HEL} and MD4 B cells, including the ability to Ig class switch, was yet to be excluded.

Failure of Anergic SW_{HEL} Double Tg B Cells to Mature and Localize to the Follicle Is Not Due to Their CSR Potential but to Competition from Nonself-reactive B Cells. To determine whether CSR potential plays any role in the impaired maturation and migration of anergic SW_{HEL} double Tg B cells, mixed radiation chimeras were produced by reconstituting ML5, AL3, and non-Tg recipients with a mixture of bone marrow cells from SW_{HEL}, MD4, and non-Tg mice. This strategy allowed the development of SW_{HEL} and MD4 HEL^+ B cells to be compared in an identical environment where they were both exposed to the same level of self-antigen and the same amount of competition from nonself-reactive B cells. In non-Tg recipients, both SW_{HEL} and MD4 HEL^+ B cells (resolved by the CD45.1 congenic marker on SW_{HEL} B cells) matured normally and contained only low frequencies of immature B cells (Fig. 6 D). In soluble HEL Tg recipients, both SW_{HEL} and MD4 HEL^+ B cells displayed a phenotype comparable to that seen in SW_{HEL} double Tg mice, with very few MZ cells being detectable (not depicted) and 40–50% of the remaining B cells expressing the immature CD21/$CD35^{lo}$ $CD23^{lo}$ phenotype (Fig. 6 D). In other words, anergic MD4 B cells also failed to mature in the presence of competitor non-Tg

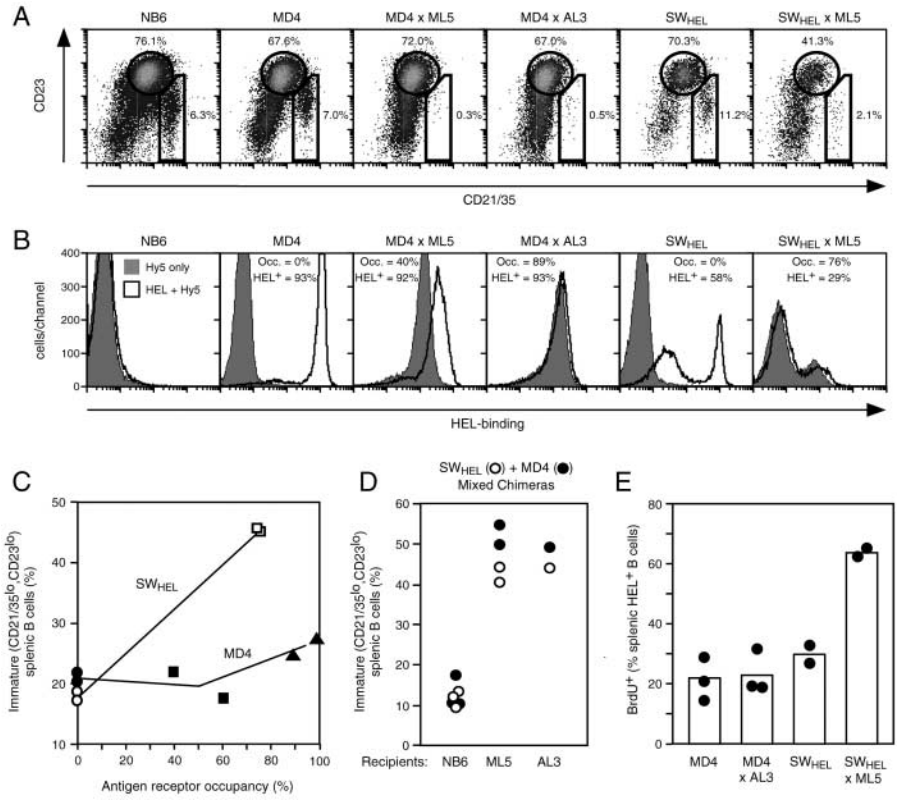

Figure 6. Anergic $SW_{HEL} \times ML5$ HEL^+ B cells have an immature phenotype and reduced lifespan due to competition with nonanergic HEL^- B cells. (A) Splenic B cell subsets in anergic and nontolerant B cell populations. Splenocytes from 9–12-wk-old mice of the indicated genotypes were stained with anti–B220-PerCP, HEL plus anti–HEL-biotin plus SA-APC, anti–CD21/CD35-FITC, and anti–CD23-PE. Data represent either total (NB6) or HEL^+ B cells (all others). Windows indicate follicular ($CD21/CD35^{int}$ $CD23^{hi}$) and MZ ($CD21/CD35^{hi}$ $CD23^{lo}$) phenotype B cells and numbers indicate the percentage of the displayed cells within these windows. (B) BCR occupancy. Splenocytes from the same mice analyzed in A were stained with anti–B220-PerCP and anti–HEL-FITC (HyHEL5) with (open histogram) and without (filled histogram) previous incubation with 200 ng/ml soluble HEL. Histograms represent anti–HEL-FITC fluorescence profiles of total ($B220^+$) B cells. To calculate receptor occupancy, HEL^+ B cells were gated (refer to Fig. 2 A) and the anti–HEL-FITC m.f.i. obtained without added HEL divided by the m.f.i. obtained with added HEL. Also indicated are the proportions of HEL^+ cells within the splenic $B220^+$ population. The low level of HEL staining on the HEL^- B cells from SW_{HEL} mice is not due to the expression of anti-HEL Ig (refer to Table I) but probably represents "cytophilic" antibody derived from the HEL^+ B cells (reference 6). For A and B, the data are representative of at least four different mice of each genotype. (C) Relationship between receptor occupancy by HEL and B cell maturation. An independent set of mice of the same genotypes and age as those described in A and B were analyzed as above. For each mouse, a receptor occupancy was calculated as was the proportion of splenic HEL^+ B cells (excluding MZ B cells) with an immature ($CD21/CD35^{lo}$ $CD23^{lo}$) phenotype. Individual data points from SW_{HEL} (○), $SW_{HEL} \times ML5$ (□), MD4 (●), $MD4 \times ML5$ (■), and $MD4 \times AL3$ (▲) are shown, with lines connecting the midpoint of duplicate data points for SW_{HEL}- and MD4-derived mice. Connecting lines serve only to indicate the trend within the SW_{HEL}- and MD4-derived mice and do not imply any linear relationship between maturation and receptor occupancy. (D) Maturation of SW_{HEL} and MD4 HEL^+ B cells exposed to the same level of HEL and B cell competition. NB6 ($n = 3$), ML5 ($n = 2$), and AL3 ($n = 1$) mice were lethally irradiated and reconstituted with a mixture of bone marrow cells from SW_{HEL}.$CD45.1^{+/-}$ (75%), MD4 (23%), and NB6 (2%) donors. After 8 wk, spleen cells from recipient mice were stained with anti–B220-PerCP, HEL plus anti–HEL-biotin plus SA-APC, anti–CD45.1-FITC, and anti–CD23-PE. After gating on small lymphocytes to exclude data from MZ B cells (confirmed by separate anti-CD21/CD35 stain), $CD45.1^+$ (SW_{HEL}) and $CD45.1^-$ (MD4) HEL^+ B cells were gated separately and the proportion of gated cells with an immature $CD23^{lo}$ phenotype were measured. Data show the readings obtained from SW_{HEL} (○) and MD4 (●) HEL^+ B cells in recipients of the indicated genotypes. (E) Relative lifespan of $SW_{HEL} \times ML5$ versus $MD4 \times AL3$ anergic B cells. Mice 9–10 wk of age of the indicated genotypes were fed BrdU via their drinking water for 72 h. Spleen cells were then stained with anti–B220-PerCP, HEL plus anti–HEL-Alexa Fluor® 647, anti–CD24-PE, and anti–BrdU-FITC. The proportion of HEL^+ B cells that stained $BrdU^+$ was calculated with reference to identically stained and analyzed spleen cells from a mouse that had not been fed BrdU. $BrdU^+$ cells were predominantly localized to the immature $CD24^{hi}$ (HSA^{hi}) compartment in all mice (not depicted), which comprised 20–30% of HEL^+ B cells in the MD4, $MD4 \times AL3$, and SW_{HEL} mice and 70–80% in the $SW_{HEL} \times ML5$ mice. Receptor occupancy was calculated as for B and was >95% in the three $MD4 \times AL3$ mice used in this experiment and 72 and 75% in the two $SW_{HEL} \times ML5$ mice.

B cells. Thus, SW_{HEL} B cells do not possess any intrinsic properties such as the ability to Ig class switch that could explain why they undergo a more severe developmental arrest than MD4 B cells on exposure to soluble self-antigen. Rather, the impairment in both maturation and follicular localization of self-reactive HEL^+ B cells in SW_{HEL} double Tg as opposed to MD4 double Tg mice is due solely to competition with the greater numbers of HEL^- B cells present in $SW_{HEL} \times ML5$ mice.

Anergic SW_{HEL} Double Tg B Cells Have a Half-Life of <3 d. Anergic MD4 B cells have been shown to have a short lifespan (half-life of <3 d) in the presence of competing HEL^- B cells (11, 27). Therefore, BrdU labeling in vivo was used to determine the relative turnover rates of HEL^+ B cells in SW_{HEL} double Tg versus SW_{HEL} mice (11, 27, 35). After 3 d of BrdU administration, >60% of self-reactive B cells from the spleens of $SW_{HEL} \times ML5$ mice were labeled with BrdU. In contrast, only ~20–30% of SW_{HEL} HEL^+ B cells were $BrdU^+$ and this labeling was confined almost exclusively to the $CD24^{hi}$ (HSA^{hi}) immature B cell pool (Fig. 6 E and not depicted). Thus, the half-life of anergic HEL^+ B cells from $SW_{HEL} \times ML5$ mice was <3 d in the spleen, which is similar to that of follicularly excluded MD4 B cells (11) and immature non-Tg B cells (36). The rate of BrdU incorporation into anergic B cells from the spleen of $MD4 \times AL3$ mice was similar to that in naive B cells from MD4 and SW_{HEL} mice (Fig. 6 E), reflecting the unchanged follicular localization and maturation of the self-

reactive B cells in these double Tg mice (Figs. 5 C and 6 A) and the relative prolongation of lifespan of anergic B cells observed in the absence of competition from nonself-reactive B cells (11).

Immature Anergic B Cells Proliferate and Secrete IgM Autoantibodies upon BCR-independent Activation. Previous experiments have shown that anergic B cells from MD4 × ML5 mice can efficiently proliferate and secrete IgM autoantibodies when activated by T cell–derived stimuli such as CD40L plus IL-4 (7, 8) or T cell–independent stimuli such as LPS (37). It is not known, however, whether immature anergic B cells excluded from the follicle can also respond to these stimuli. To test this, small resting splenic B cells were purified from SW_{HEL} and SW_{HEL} × ML5 mice, labeled with the division-tracking dye CFSE, and cultured in vitro with the BCR-independent stimuli anti-CD40 mAb plus IL-4 (Figs. 7 and 9) and LPS (Figs. 8 and 10).

Proliferation of the various B cell populations was visualized by monitoring the serial twofold reductions in CFSE fluorescence intensity that accompany cell division (26). When responses to anti-CD40 mAb plus IL-4 were examined, nontolerant HEL^+ SW_{HEL} B cells proliferated less than both HEL^- SW_{HEL} B cells and non-Tg B cells (Fig. 7, A and B). Thus, a greater proportion of the HEL^+ SW_{HEL} B cells either failed to divide or underwent only a few cell divisions after 4 d in culture. Proliferation by MD4 B cells was similar, indicating that small resting Tg B cells expressing the HyHEL10 specificity respond less efficiently to anti-CD40 mAb plus IL-4 than non-Tg B cells. On the other hand, anergic B cells from both SW_{HEL} × ML5 (Fig. 7, A and B) and MD4 × ML5 mice (not depicted) responded better than the corresponding nontolerant B cells, with proliferation being comparable to that of non-Tg B cells. Because the anergic B cells had matured in the presence of HEL, this finding underscored the role of the BCR in modulating responsiveness to this T-dependent stimulus. By contrast, proliferative responses to the T-independent stimulus LPS did not vary greatly between the different B cell populations and were identical for HEL^+ SW_{HEL} single and double Tg B cells (Fig. 8, A and B). Both anti-CD40 mAb plus IL-4 as well as LPS elicited comparable amounts of anti-HEL IgM antibodies from anergic and nontolerant HEL^+ SW_{HEL} B cells (Figs. 7 C and 8 C). Thus, proliferation and production of IgM autoantibodies in response to these BCR-independent stimuli are not reduced in immature, follicularly excluded anergic B cells.

Immature Anergic B Cells Undergo CSR and Secrete IgG Autoantibodies upon BCR-independent Activation. To test whether anergic B cells are intrinsically compromised in their ability to undergo CSR, naive and anergic SW_{HEL} B cells were cultured in parallel with C57BL/6 and MD4 B cells and then analyzed for production of IgG1 and IgG3 in response to anti-CD40 mAb plus IL-4 (Fig. 9) and LPS (Fig. 10) respectively. Flow cytometric analysis of surface expression of IgG revealed that both SW_{HEL} and SW_{HEL} × ML5 HEL^+ B cells switched efficiently to IgG1 and IgG3 whereas minimal switching occurred in MD4 B cells (Figs. 9, A and B, and 10, A and B). When the proportions of $IgG1^+$ B cells in each cell division were calculated, SW_{HEL} and SW_{HEL} × ML5 HEL^+ B cells were found to have identical cell division–dependent patterns of IgG1 switching (Fig. 9 B). The same was true for switching to IgG3 in response to LPS (Fig. 10 B). ELISA of culture supernatant for secretion of anti-HEL IgG1 and IgG3 antibodies mirrored the degree of switching observed by flow cytometry. That is, the anergic SW_{HEL} B cells in each case

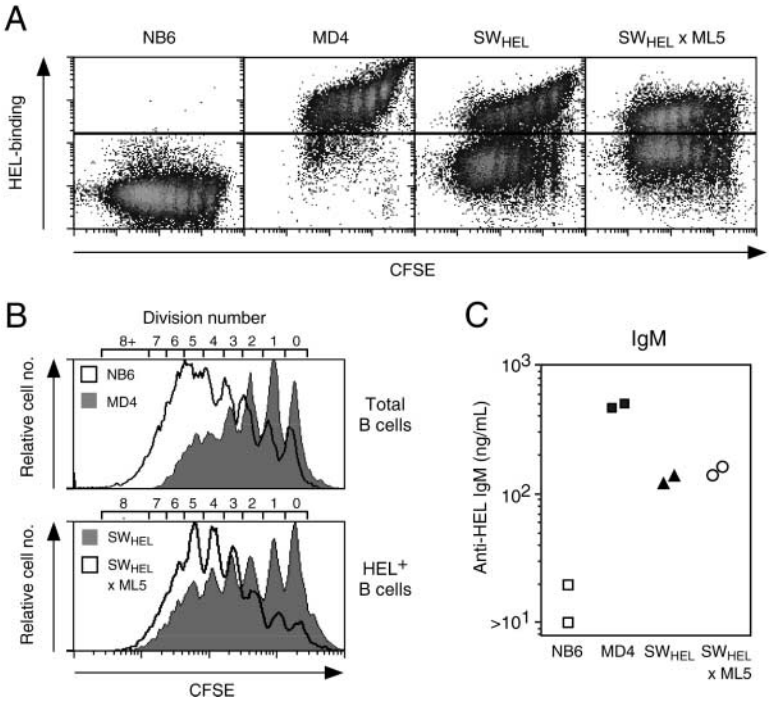

Figure 7. Anergic SW_{HEL} B cells readily proliferate and secrete IgM autoantibodies in response to T cell–derived signals. CFSE-labeled small resting B cells purified from 8–12-wk-old NB6, MD4, SW_{HEL}, and SW_{HEL} × ML5 mice were stimulated in vitro with anti-CD40 mAb plus IL-4 for 4 d. Cells were then fixed, permeabilized, and stained with HEL plus anti–HEL-Alexa Flour® 647. (A) Density plot of HEL binding versus CFSE cell division profile for mice of the indicated genotypes. (B) Overlays of CFSE cell division profiles demonstrating the lower proliferative responses of MD4 and HEL^+ SW_{HEL} B cells compared with NB6 B cells and HEL^+ SW_{HEL} × ML5 B cells. HEL^- B cells from SW_{HEL} and SW_{HEL} × ML5 mice exhibited CFSE profiles similar to that of NB6 B cells (A and not depicted). The number of divisions undergone by cells in specific CFSE peaks is indicated. Note that peaks do not exactly correspond between samples due to minor differences in CFSE labeling efficiency. (C) Secretion of IgM anti-HEL antibodies by NB6, MD4, SW_{HEL}, and SW_{HEL} × ML5 B cells. Duplicate cultures of purified B cells were stimulated in vitro with anti-CD40 mAb plus IL-4 and anti-HEL IgM detected by ELISA of culture supernatants. Data are representative of four independent experiments.

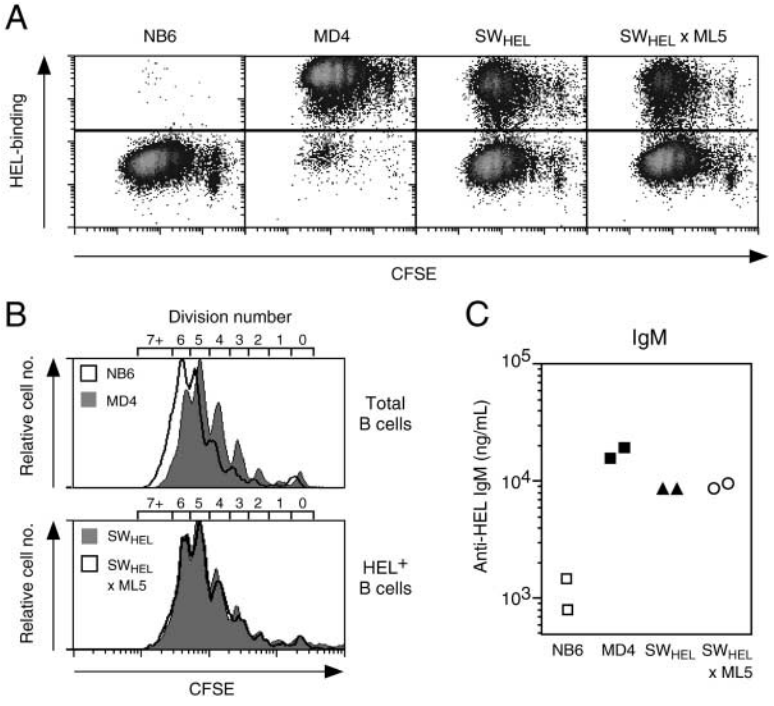

Figure 8. Anergic SW_{HEL} B cells readily proliferate and secrete IgM autoantibodies in response to LPS. CFSE-labeled small resting B cells purified from 8–12-wk-old NB6, MD4, SW_{HEL}, and $SW_{HEL} \times$ ML5 mice were stimulated in vitro with LPS for 3 d. Cells were then fixed, permeabilized, and stained with HEL plus anti–HEL-Alexa Flour® 647. (A) Density plot of HEL binding versus CFSE cell division profile for mice of the indicated genotypes. (B) Overlays of CFSE cell division profiles demonstrating the slightly lower proliferative responses of MD4, SW_{HEL} HEL^+, and $SW_{HEL} \times$ ML5 HEL^+ B cells compared with NB6 B cells. HEL^- B cells from SW_{HEL} and $SW_{HEL} \times$ ML5 mice exhibited CFSE profiles identical to that of NB6 B cells (A and not depicted). The number of divisions undergone by cells in specific CFSE peaks are indicated. Note that peaks do not exactly correspond between samples due to minor differences in CFSE labeling efficiency. (C) Secretion of IgM anti-HEL antibodies by NB6, MD4, SW_{HEL}, and $SW_{HEL} \times$ ML5 B cells. Duplicate cultures of purified B cells were stimulated in vitro with LPS and anti-HEL IgM detected by ELISA of culture supernatants. Data are representative of four independent experiments.

produced at least as much anti-HEL IgG antibody as the nontolerant SW_{HEL} B cells (Figs. 9 C and 10 C). Therefore, anergic B cells have no intrinsic block to CSR nor to subsequent secretion of potentially pathogenic IgG1 or IgG3 autoantibodies.

Discussion

The MD4 Ig Tg model has been used for more than a decade to study the regulation of B cell responses, both in tolerance and immunity. With the development of SW_{HEL} mice, it is now possible to extend the observations made in the original model to encompass the full range of B cell responses. This is due primarily to the ability of HEL^+ B cells from SW_{HEL} but not MD4 mice to undergo CSR to all Ig isotypes (Fig. 3, A and B). Although SW_{HEL} mice will be valuable for future studies of B cell memory, plasma cell development and other aspects of late B cell differentiation, we have used them initially to investigate the effect of the anergic state on CSR. The experiments described here show for the first time that CSR and secretion of IgG autoantibodies are not intrinsically blocked after induction of tolerance in B cells.

Comparison of SW_{HEL} with MD4 mice revealed that the phenotypes of naive HEL^+ B cells from the two lines are very similar. Both populations of B cells are restricted to the B2 lineage (Fig. 2 C), migrate to the splenic follicle and MZ (Fig. 5, A and D), and share the same differential expression of B cell surface markers such as CD21/CD35 and CD23 (Fig. 6 A). In addition, SW_{HEL} and MD4 HEL^+ B cells express uniformly high levels of surface IgM (Fig. 2 B) regardless of their CD21/CD35 and CD23 surface phenotype or anatomical localization in the spleen. Although MZ B cells are also IgM^{hi} in non-Tg mice, the long-lived recirculating and follicular B cell pool normally exhibits a range from low to high expression of surface IgM (38). The absence of IgM^{lo} follicular HEL^+ B cells cannot be ascribed to trivial factors such as transgene copy number or integration site because it occurs in both SW_{HEL} and MD4 mice. Rather, the established role of BCR specificity in shaping the differentiation of maturing B cells (39) suggests instead that the uniformly IgM^{hi} phenotype of HEL^+ follicular B cells reflects the unique interactions of the HyHEL10 BCR specificity with the endogenous antigenic milieu.

Apart from the ability to undergo CSR, SW_{HEL} mice are also distinguished from MD4 Ig Tg mice by the presence of significant numbers of HEL^- B cells (Fig. 2 A). This difference is due to the targeted insertion of the V_H10 heavy chain gene into the IgH locus in the SW_{HEL} mice that allows replacement of the rearranged V_H segment by upstream V_H or V_H plus D elements during early B cell development (Table I and not depicted). Consistent with results from other mice carrying targeted V_HDJ_H genes (22, 23), recombination events in SW_{HEL} mice are mediated by the embedded RSS heptamer located at the 3′ end of the rearranged V_H segment of V_H10 (not depicted). In mice carrying a targeted insertion of an anti-DNA V_HDJ_H gene, this phenomenon may represent a receptor-editing mechanism activated in response to the binding of self-antigen (22). Such a scenario is unlikely in SW_{HEL} mice however, because anti-HEL B cells show no evidence of self-reactivity in the absence of transgenically expressed HEL and undergo profound changes when HEL is expressed as a soluble- or membrane-bound self-antigen (2, 5–11, and this study). Therefore, it is more likely that the V_H replacement events in SW_{HEL} mice reflect a general instability of rear-

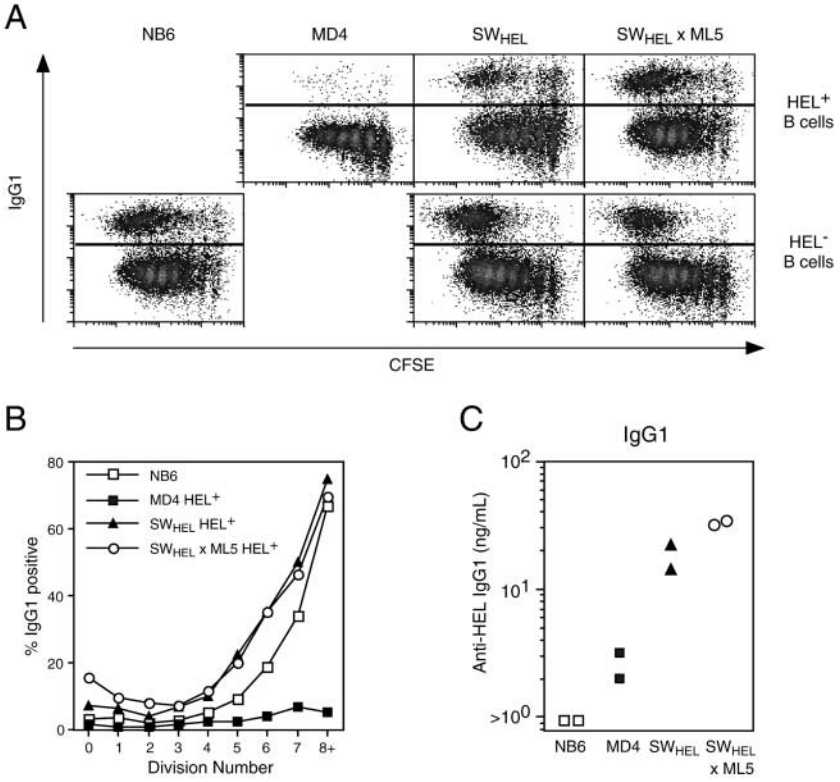

Figure 9. Anergic SW_{HEL} B cells readily class switch and secrete IgG1 autoantibodies in response to T cell–derived signals. CFSE-labeled small resting B cells were prepared, stimulated, and stained as in Fig. 7 with an additional stain of anti–IgG1-biotin plus SA-PE. Data were gated on HEL^+ and HEL^- B cells using the regions shown in Fig. 7 A. (A) Density plot of IgG1 expression versus CFSE cell division profile for HEL^+ (top) and HEL^- B cells (bottom) from mice of the indicated genotypes. (B) Analysis of switching per cell division. Gates were drawn around each CFSE peak as shown in Fig. 7 B to determine the cell division number and the percentage of $IgG1^+$ cells in each division calculated by backgating using the region shown in A. NB6 (□), HEL^+ MD4 (■), HEL^+ SW_{HEL} (▲), and HEL^+ SW_{HEL} × ML5 B cells (○) are shown. HEL^- B cells from SW_{HEL} and SW_{HEL} × ML5 mice had comparable profiles to NB6 (A and not depicted). (C) Secretion of IgG1 anti-HEL antibodies by NB6, MD4, SW_{HEL}, and SW_{HEL} × ML5 B cells. Duplicate cultures of purified B cells were stimulated in vitro with anti-CD40 mAb plus IL-4 and anti-HEL IgG1 detected by ELISA of culture supernatants. Data are representative of four independent experiments.

ranged V_HDJ_H genes during early B cell development before the down-regulation of the RAG recombinases.

The presence of HEL^- B cells in SW_{HEL} but not MD4 Ig Tg mice became of particular relevance when the two lines of mice were crossed with mice expressing soluble HEL. The resulting populations of self-reactive B cells were anergic as indicated by surface IgM down-regulation (Fig. 4 B and not depicted), low levels of antibody secretion in vivo

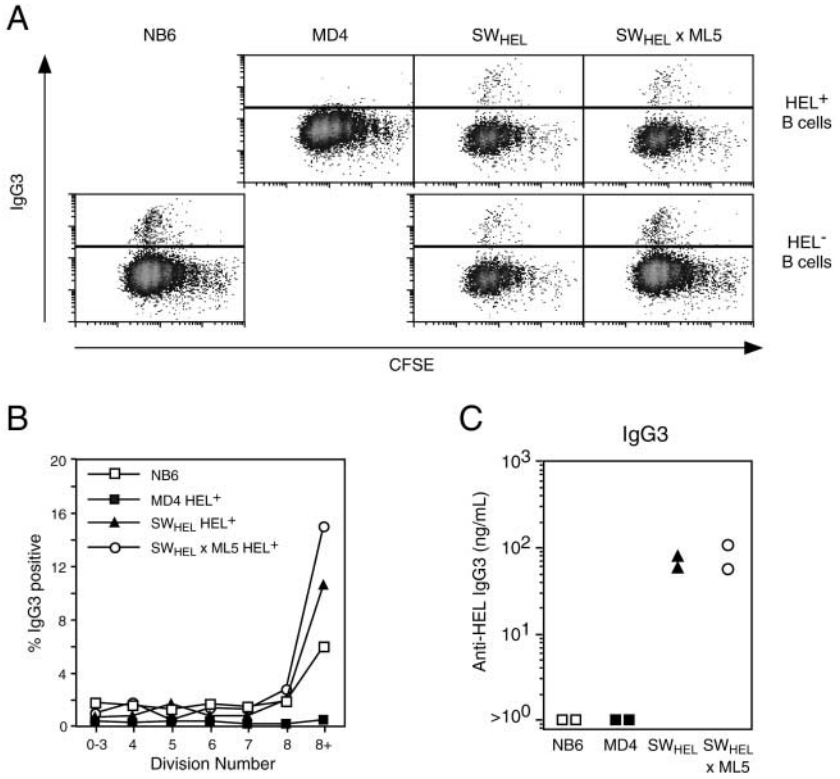

Figure 10. Anergic SW_{HEL} B cells readily class switch and secrete IgG3 autoantibodies in response to LPS. CFSE-labeled small resting B cells were prepared, stimulated, and stained as in Fig. 8 with an additional stain of anti–IgG3-biotin plus SA-PE. Data were gated on HEL^+ and HEL^- B cells using the regions shown in Fig. 8 A. (A) Density plot of IgG3 expression versus CFSE cell division profile for HEL^+ (top) and HEL^- B cells (bottom) from mice of the indicated genotypes. (B) Analysis of switching per cell division. Gates were drawn around each CFSE peak as shown in Fig. 8 B to determine the cell division number and the percentage of $IgG3^+$ cells in each division calculated by backgating using the region shown in A. NB6 (□), HEL^+ MD4 (■), HEL^+ SW_{HEL} (▲), and HEL^+ SW_{HEL} × ML5 B cells (○) are shown. HEL^- B cells from SW_{HEL} and SW_{HEL} × ML5 mice had comparable profiles to NB6 (A and not depicted). (C) Secretion of IgG3 anti-HEL antibodies by NB6, MD4, SW_{HEL}, and SW_{HEL} × ML5 B cells. Duplicate cultures of purified B cells were stimulated in vitro with LPS and anti-HEL IgG3 detected by ELISA of culture supernatants. Data are representative of four independent experiments.

(Fig. 4 C), and loss of BCR signaling capabilities (Fig. 4 D). However, in contrast to the anergic B cells from MD4 double Tg mice, self-reactive SW_{HEL} double Tg B cells were present at reduced frequencies (Fig. 4 A), arrested in their migration at the outer PALS (Fig. 5 E), failed to mature (Fig. 6, A and C), and exhibited a shortened life-span (Fig. 6 E). The demonstration that the differences in phenotype between the two types of anergic B cells are due solely to the presence of competitor B cells in the SW_{HEL} mice has finally resolved a long-standing point of controversy surrounding the fate of anergic B cells.

This controversy has stemmed from independent studies based on the original anti-HEL double Tg model that have given rise to two differing theories as to why follicular exclusion and reduced survival of anergic B cells occur in the presence of nonself-reactive B cells. On the one hand it has been argued that anergic B cells compete poorly with nonself-reactive B cells for essential migratory and survival signals (11, 12). Alternatively, the relative increase in available self-antigen accompanying reduced frequencies of HEL^+ B cells, as observed in $SW_{HEL} \times$ ML5 versus MD4 $\times$ ML5 mice (Fig. 6 B), may provide anergic B cells with a stronger BCR signal leading in turn to outer PALS arrest and shortened lifespan (13). In support of this interpretation is the previous demonstration of outer PALS arrest in some MD4 $\times$ AL3 mice and in MD4 $\times$ ML5 mice induced to secrete higher levels of HEL (13).

Simultaneous measurement of competitor (HEL^-) B cell frequency and receptor occupancy (Fig. 6 B) was combined with analysis of mixed bone marrow chimeras (Fig. 6 D) to clearly demonstrate that the impaired migration, maturation, and survival of anergic SW_{HEL} B cells is due to competition with HEL^- B cells. Critical to this conclusion was that the MD4 $\times$ AL3 mice examined in the current experiments contained $<$10% HEL^- B cells and possessed anergic HEL^+ B cells that had 90–100% saturation of their BCRs with self-antigen (Fig. 6, B and C). Nonetheless, these anergic MD4 $\times$ AL3 B cells survived at normal frequencies (Fig. 4 A), colonized the follicle (Fig. 5 C), matured normally to the follicular stage (Fig. 6 A), and had a normal lifespan (Fig. 6 E). The discrepancy between our results and those obtained by Cook et al. (13) almost certainly relates to the older age of the mice used in their experiments compared with ours (4–9 mo vs. 8–12 wk) because HEL^- B cells accumulate with age (27) and are clearly present at high frequencies in the mice used in their experiments (13). Therefore, maximal signaling by soluble HEL is insufficient in itself to exclude anergic B cells from the follicle and competition from nonself-reactive B cells is necessary for this to occur.

Although the induction of anergy and follicular exclusion can be achieved independently by manipulating the amount of competition from nonself-reactive B cells (11), anergy and follicular exclusion are in fact likely to be coincident in the normal B cell repertoire where competition is always present. Therefore, many if not all anergic B cells generated in the normal repertoire might be immature and behave in a similar way to those in the new SW_{HEL} double Tg model rather than the original MD4 double Tg model. Thus, as is observed in SW_{HEL} double Tg mice, self-reactive B cells that lack sufficient avidity to be deleted in the bone marrow are likely to be eliminated from the long-lived peripheral B cell pool by competition from nonself-reactive B cells (12). What then is the basis for competitive exclusion of anergic B cells from the long-lived peripheral B cell pool? If survival of immature B cells is contingent on their migration into the follicle, one possibility is that anergic B cells fail to compete efficiently for the follicular chemokine CXCL13 (BLC; reference 40). In support of this notion, anergic B cells with anti-DNA specificity that localize to the outer PALS express low levels of the CXCL13 receptor CXCR5 (BLR1; reference 41). Alternatively, anergic B cells may not compete effectively for signals mediated by the TNF family ligand BAFF because B cells from $BAFF^{-/-}$ mice have an immature phenotype resembling that of SW_{HEL} double Tg B cells (42).

Because anergic B cells present in the normal repertoire not only have the potential to undergo CSR but are likely to be immature, the availability of the SW_{HEL} double Tg mice with a similar immature phenotype makes it timely to reevaluate the physiological relevance of the findings obtained in the original model. For instance, the immature phenotype could be associated with poor responsiveness to BCR-independent stimuli (43) compared to the behavior of MD4 double Tg B cells (7, 8, 37). Nevertheless, this proved not to be the case because the responsiveness of SW_{HEL} double Tg B cells to anti-CD40 mAb plus IL-4 (Fig. 7) and LPS (Fig. 8) clearly showed that immature anergic B cells retain the ability to proliferate and secrete anti-HEL IgM autoantibodies when activated by BCR-independent stimuli. Moreover, the switching capability of SW_{HEL} B cells enabled us to study for the first time whether anergic B can undergo CSR. Given that IgG autoantibodies are more pathogenic (15–19) and less prevalent (20) than IgM autoantibodies, we anticipated that intrinsic controls over Ig class switching would be required to reinforce peripheral B cell self-tolerance and prevent autoimmunity. Surprisingly, anergic SW_{HEL} B cells were shown to undergo efficient isotype switching and secrete IgG1 and IgG3 autoantibodies when they were activated independently of the BCR with both T cell–derived (Fig. 9) and T-independent (Fig. 10) stimuli.

The lack of intrinsic controls over CSR and secretion of IgG by anergic B cells highlights the need to impose additional controls on these cells to prevent their activation by BCR-independent stimuli. In the case of T cell–dependent signals, the requirement for BCR-mediated CD86 up-regulation to facilitate delivery of productive T cell help (44, 45), and the abrogation of this in anergic B cells (Fig. 4 D), means that T cell–derived signals such as CD40L plus IL-4 are unlikely to induce IgG production by anergic B cells under normal circumstances. In contrast, type I T-independent stimuli such as LPS activate B cells in the absence of BCR engagement, meaning that access to such stimuli by self-reactive B cells must be restricted to prevent IgG autoantibody production. Two ways in which this appears to

be achieved were shown here for SW_{HEL} double Tg B cells. The first involved limiting the survival of anergic B cells in the periphery (Fig. 6 E). Second, the restriction of their migration into the splenic follicle and MZ reduces the possibility of contact with type I T-independent stimuli. In this regard, the purging of self-reactive B cells from the MZ is likely to be particularly important because blood-borne pathogens (such as Gram-negative bacteria bearing LPS) are directly filtered through the MZ via the marginal sinus (46). Significantly, although the inhibition of maturation, survival, and follicular homing by anergic B cells depends on the presence of competitor B cells, the purging of anergic B cells from the MZ does not (Fig. 5), suggesting that this aspect of anergic B cell regulation is fundamental to B cell self-tolerance.

Therefore, how are pathogenic IgG autoantibodies produced? Based on the data presented here, any perturbation that increases the chances of self-reactive B cells coming into contact with type I T-independent stimuli may facilitate the production of IgG autoantibodies. This would include mutations that either increase the lifespan of anergic B cells or their entry into microenvironments from which they are normally excluded. As discussed above, the accumulation of self-reactive B cells in the MZ would be particularly dangerous. Interestingly, many models of antibody-mediated autoimmune diseases, including estrogen-induced lupus (47), the NZB/NZW F1 lupus model (48), and the BAFF-Tg model of Sjögren's syndrome (49), have established correlations between the onset of disease and an expanded MZ compartment. Our data also suggest that acute exposure to LPS may trigger IgG production by anergic B cells despite their restricted lifespan and migration. This is consistent with previous studies showing that LPS administration results in the secretion of pathogenic IgG autoantibodies, induction of nephritis in normal mice, and exacerbation of nephritis in lupus-prone mice (50–52). A similar mechanism may underlie the long-recognized association between systemic infection and clinical relapses of lupus (53). Exposure of anergic B cells to LPS may not only induce production of IgG autoantibodies directly. Through its ability to up-regulate CD86 expression on B cells (54), LPS may circumvent the BCR signaling deficiency of anergic B cells and facilitate their T cell–dependent activation (44, 45). As demonstrated here, T cell–dependent activation by CD40L plus IL-4 delivered in this scenario would indeed trigger subsequent production of IgG autoantibodies (Fig. 9).

We thank Jenny Kingham, Chris Brownlee, and the staff of the Centenary Institute Animal Facility for animal husbandry, Tyani Chan for mouse screening, and Joseph Webster and Tara MacDonald for FACS® sorting. We also thank Dr. Sigrid Ruuls for generously providing the loxP-neo^r-loxP cassette and Drs. Stephen Adelstein, Barbara Fazekas de St. Groth, and Stuart Tangye for their critical discussions and review of the manuscript.

This work was supported by a program grant from the National Health and Medical Research Council of Australia. T.G. Phan received a National Health and Medical Research Council postgraduate research scholarship.

Submitted: 16 December 2002
Revised: 24 January 2003
Accepted: 5 February 2003

References

1. Nemazee, D., and K. Buerki. 1989. Clonal deletion of autoreactive B lymphocytes in bone marrow chimeras. *Proc. Natl. Acad. Sci. USA.* 86:8039–8043.
2. Hartley, S.B., J. Crosbie, R. Brink, A.B. Kantor, A. Basten, and C.C. Goodnow. 1991. Elimination from peripheral lymphoid tissues of self-reactive B lymphocytes recognizing membrane-bound antigens. *Nature.* 353:765–769.
3. Radic, M.Z., J. Erikson, S. Litwin, and M. Weigert. 1993. B lymphocytes may escape tolerance by revising their antigen receptors. *J. Exp. Med.* 177:1165–1173.
4. Tiegs, S.L., D.M. Russell, and D. Nemazee. 1993. Receptor editing in self-reactive bone marrow B cells. *J. Exp. Med.* 177:1009–1020.
5. Goodnow, C.C., J. Crosbie, S. Adelstein, T.B. Lavoie, S.J. Smith-Gill, R.A. Brink, H. Pritchard-Briscoe, J.S. Wotherspoon, R.H. Loblay, K. Raphael, et al. 1988. Altered immunoglobulin expression and functional silencing of self-reactive B lymphocytes in transgenic mice. *Nature.* 334:676–682.
6. Mason, D.Y., M. Jones, and C.C. Goodnow. 1992. Development and follicular localization of tolerant B lymphocytes in lysozyme/anti-lysozyme IgM/IgD transgenic mice. *Int. Immunol.* 4:163–175.
7. Eris, J.M., A. Basten, R. Brink, K. Doherty, M.R. Kehry, and P.D. Hodgkin. 1994. Anergic self-reactive B cells present self antigen and respond normally to CD40-dependent T-cell signals but are defective in antigen-receptor-mediated functions. *Proc. Natl. Acad. Sci. USA.* 91:4392–4396.
8. Cooke, M.P., A.W. Heath, K.M. Shokat, Y. Zeng, F.D. Finkelman, P.S. Linsley, M. Howard, and C.C. Goodnow. 1994. Immunoglobulin signal transduction guides the specificity of B cell–T cell interactions and is blocked in tolerant self-reactive B cells. *J. Exp. Med.* 179:425–438.
9. Healy, J.I., R.E. Dolmetsch, L.A. Timmerman, J.G. Cyster, M.L. Thomas, G.R. Crabtree, R.S. Lewis, and C.C. Goodnow. 1997. Different nuclear signals are activated by the B cell receptor during positive versus negative signaling. *Immunity.* 6:419–428.
10. Glynne, R., G. Ghandour, J. Rayner, D.H. Mack, and C.C. Goodnow. 2000. B-lymphocyte quiescence, tolerance and activation as viewed by global gene expression profiling on microarrays. *Immunol. Rev.* 176:216–246.
11. Cyster, J.G., and C.C. Goodnow. 1995. Antigen-induced exclusion from follicles and anergy are separate and complementary processes that influence peripheral B cell fate. *Immunity.* 3:691–701.
12. Cyster, J.G., S.B. Hartley, and C.C. Goodnow. 1994. Competition for follicular niches excludes self-reactive cells from the recirculating B-cell repertoire. *Nature.* 371:389–395.
13. Cook, M.C., A. Basten, and B. Fazekas De St Groth. 1997. Outer periarteriolar lymphoid sheath arrest and subsequent differentiation of both naive and tolerant immunoglobulin transgenic B cells is determined by B cell receptor occupancy. *J. Exp. Med.* 186:631–643.
14. Goldsby, R.A., T.J. Kindt, and B.A. Osborne. 2000. Immunoglobulins: structure and function. *In* Kuby Immunology. R.A. Goldsby, T.J. Kindt, and B.A. Osborne, editors. W.H. Freeman and Company, New York. 95–96.

15. Steward, M.W., and F.C. Hay. 1976. Changes in immunoglobulin class and subclass of anti-DNA antibodies with increasing age in N/ZBW F1 hybrid mice. *Clin. Exp. Immunol.* 26:363–370.
16. Papoian, R., R. Pillarisetty, and N. Talal. 1977. Immunological regulation of spontaneous antibodies to DNA and RNA. II. Sequential switch from IgM to IgG in NZB/NZW F1 mice. *Immunology.* 32:75–79.
17. Panosian-Sahakian, N., J.L. Klotz, F. Ebling, M. Kronenberg, and B. Hahn. 1989. Diversity of Ig V gene segments found in anti-DNA autoantibodies from a single (NZB × NZW)F1 mouse. *J. Immunol.* 142:4500–4506.
18. Tillman, D.M., N.T. Jou, R.J. Hill, and T.N. Marion. 1992. Both IgM And IgG anti-DNA antibodies are the products of clonally selective B cell stimulation in (NZB × NZW)F1 mice. *J. Exp. Med.* 176:761–779.
19. Peng, S.L., S.J. Szabo, and L.H. Glimcher. 2002. T-Bet regulates IgG class switching and pathogenic autoantibody production. *Proc. Natl. Acad. Sci. USA.* 99:5545–5550.
20. George, J., and Y. Shoenfeld. 1996. Natural autoantibodies. *In* Autoantibodies. J.B. Peter and Y. Shoenfeld, editors. Elsevier, Amsterdam. 534–539.
21. Taki, S., M. Meiering, and K. Rajewsky. 1993. Targeted insertion of a variable region gene into the immunoglobulin heavy chain locus. *Science.* 262:1268–1271.
22. Chen, C., Z. Nagy, E.L. Prak, and M. Weigert. 1995. Immunoglobulin heavy chain gene replacement: a mechanism of receptor editing. *Immunity.* 3:747–755.
23. Cascalho, M., A. Ma, S. Lee, L. Masat, and M. Wabl. 1996. A quasi-monoclonal mouse. *Science.* 272:1649–1652.
24. Hartley, S.B., and C.C. Goodnow. 1994. Censoring of self-reactive B cells with a range of receptor affinities in transgenic mice expressing heavy chains for a lysozyme-specific antibody. *Int. Immunol.* 6:1417–1425.
25. Lemckert, F.A., J.D. Sedgwick, and H. Korner. 1997. Gene targeting in C57BL/6 ES cells. Successful germ line transmission using recipient Balb/C blastocysts developmentally matured in vitro. *Nucleic Acids Res.* 25:917–918.
26. Lyons, A.B., and C.R. Parish. 1994. Determination of lymphocyte division by flow cytometry. *J. Immunol. Methods.* 171:131–137.
27. Fulcher, D.A., and A. Basten. 1994. Reduced life span of anergic self-reactive B cells in a double-transgenic model. *J. Exp. Med.* 179:125–134.
28. Hodgkin, P.D., and M.R. Kehry. 1996. Methods for polyclonal B lymphocyte activation to proliferation and Ig secretion *in vitro*. *In* Weir's Handbook of Experimental Immunology. L.A. Herzenberg, D.M. Weir, and C. Blackwell, editors. Blackwell Science, Cambridge. 89.1–13.
29. Gerstein, R.M., W.N. Frankel, C.L. Hsieh, J.M. Durdik, S. Rath, J.M. Coffin, A. Nisonoff, and E. Selsing. 1990. Isotype switching of an immunoglobulin heavy chain transgene occurs by DNA recombination between different chromosomes. *Cell.* 63:537–548.
30. Deenick, E.K., J. Hasbold, and P.D. Hodgkin. 1999. Switching to IgG3, IgG2b, and IgA is division linked and independent, revealing a stochastic framework for describing differentiation. *J. Immunol.* 163:4707–4714.
31. Hasbold, J., J.S. Hong, M.R. Kehry, and P.D. Hodgkin. 1999. Integrating signals from IFN-gamma and IL-4 by B cells: positive and negative effects on CD40 ligand-induced proliferation, survival, and division-linked isotype switching to IgG1, IgE, and IgG2a. *J. Immunol.* 163:4175–4181.
32. Waldschmidt, T.J., D.H. Conrad, and R.G. Lynch. 1988. The expression of B cell surface receptors. I. The ontogeny and distribution of the murine B cell IgE Fc receptor. *J. Immunol.* 140:2148–2154.
33. Takahashi, K., Y. Kozono, T.J. Waldschmidt, D. Berthiaume, R.J. Quigg, A. Baron, and V.M. Holers. 1997. Mouse complement receptors type 1 (Cr1;CD35) and type 2 (Cr2; CD21): expression on normal B cell subpopulations and decreased levels during the development of autoimmunity in MRL/Lpr mice. *J. Immunol.* 159:1557–1569.
34. Oliver, A.M., F. Martin, G.L. Gartland, R.H. Carter, and J.F. Kearney. 1997. Marginal zone B cells exhibit unique activation, proliferative and immunoglobulin secretory responses. *Eur. J. Immunol.* 27:2366–2374.
35. Forster, I., and K. Rajewsky. 1990. The bulk of the peripheral B-cell pool in mice is stable and not rapidly renewed from the bone marrow. *Proc. Natl. Acad. Sci. USA.* 87:4781–4784.
36. Fulcher, D.A., and A. Basten. 1997. Influences on the lifespan of B cell subpopulations defined by different phenotypes. *Eur. J. Immunol.* 27:1188–1199.
37. Goodnow, C.C., R. Brink, and E. Adams. 1991. Breakdown of self-tolerance in anergic B lymphocytes. *Nature.* 352:532–536.
38. Hao, Z., and K. Rajewsky. 2001. Homeostasis of peripheral B cells in the absence of B cell influx from the bone marrow. *J. Exp. Med.* 194:1151–1164.
39. Hardy, R.R., and K. Hayakawa. 2001. B cell development pathways. *Annu. Rev. Immunol.* 19:595–621.
40. Gunn, M.D., V.N. Ngo, K.M. Ansel, E.H. Ekland, J.G. Cyster, and L.T. Williams. 1998. A B-cell-homing chemokine made in lymphoid follicles activates Burkitt's lymphoma receptor-1. *Nature.* 391:799–803.
41. Seo, S.J., M.L. Fields, J.L. Buckler, A.J. Reed, L. Mandik-Nayak, S.A. Nish, R.J. Noelle, L.A. Turka, F.D. Finkelman, A.J. Caton, et al. 2002. The impact of T helper and T regulatory cells on the regulation of anti-double-stranded DNA B cells. *Immunity.* 16:535–546.
42. Schiemann, B., J.L. Gommerman, K. Vora, T.G. Cachero, S. Shulga-Morskaya, M. Dobles, E. Frew, and M.L. Scott. 2001. An essential role for BAFF in the normal development of B cells through a BCMA-independent pathway. *Science.* 293:2111–2114.
43. Rolink, A.G., J. Andersson, and F. Melchers. 1998. Characterization of immature B cells by a novel monoclonal antibody, by turnover and by mitogen reactivity. *Eur. J. Immunol.* 28:3738–3748.
44. Rathmell, J.C., S.E. Townsend, J.C. Xu, R.A. Flavell, and C.C. Goodnow. 1996. Expansion or elimination of B cells in vivo: dual roles for CD40- and Fas (CD95)-ligands modulated by the B cell antigen receptor. *Cell.* 87:319–329.
45. Rathmell, J.C., S. Fournier, B.C. Weintraub, J.P. Allison, and C.C. Goodnow. 1998. Repression of B7.2 on self-reactive B cells is essential to prevent proliferation and allow Fas-mediated deletion by $CD4^+$ T cells. *J. Exp. Med.* 188:651–659.
46. Cyster, J.G. 2000. B cells on the front line. *Nat. Immunol.* 1:9–10.
47. Grimaldi, C.M., D.J. Michael, and B. Diamond. 2001. Cutting edge: expansion and activation of a population of autoreactive marginal zone B cells in a model of estrogen-induced lupus. *J. Immunol.* 167:1886–1890.
48. Wellmann, U., A. Werner, and T.H. Winkler. 2001. Altered

selection processes of B lymphocytes in autoimmune NZB/W mice, despite intact central tolerance against DNA. *Eur. J. Immunol.* 31:2800–2810.
49. Groom, J., S.L. Kalled, A.H. Cutler, C. Olson, S.A. Woodcock, P. Schneider, J. Tschopp, T.G. Cachero, M. Batten, J. Wheway, et al. 2002. Association of BAFF/BLys overexpression and altered B cell differentiation with Sjögren's syndrome. *J. Clin. Invest.* 109:59–68.
50. Hang, L., J.H. Slack, C. Amundson, S. Izui, A.N. Theofilopoulos, and F.J. Dixon. 1983. Induction of murine autoimmune disease by chronic polyclonal B cell activation. *J. Exp. Med.* 157:874–883.
51. Cavallo, T., and N.A. Granholm. 1990. Lipopolysaccharide from gram-negative bacteria enhances polyclonal B cell activation and exacerbates nephritis in MRL/Lpr mice. *Clin. Exp. Immunol.* 82:515–521.
52. Granholm, N.A., and T. Cavallo. 1992. Autoimmunity, polyclonal B-cell activation and infection. *Lupus.* 1:63–74.
53. Wallace, D.J., and E.L. Dubois. 1987. Prognostic subsets, natural course, and causes of death in systemic lupus erythematosus. *In* Dubois' Lupus Erythematosus. D.J. Wallace and E.L. Dubois, editors. Lea & Febiger, Philadelphia. 583–584.
54. Hathcock, K.S., G. Laszlo, C. Pucillo, P. Linsley, and R.J. Hodes. 1994. Comparative analysis of B7-1 and B7-2 costimulatory ligands: expression and function. *J. Exp. Med.* 180: 631–640.